

# THE ISOTOPE EFFECT IN SUPERCONDUCTORS

A. Bill,<sup>1</sup> V.Z. Kresin,<sup>1</sup> and S.A. Wolf<sup>2</sup>

<sup>1</sup> Lawrence Berkeley Laboratory, University of California,  
Berkeley, CA 94720, USA

<sup>2</sup> Naval Research Laboratory, Washington D.C. 20375-5343

## Abstract

We review some aspects of the isotope effect (IE) in superconductors. Our focus is on the influence of factors not related to the pairing mechanism. After summarizing the main results obtained for conventional superconductors, we review the effect of magnetic impurities, the proximity effect and non-adiabaticity on the value of the isotope coefficient (IC). We discuss the isotope effect of  $T_c$  and of the penetration depth  $\delta$ . The theory is applied to conventional and high- $T_c$  superconductors. Experimental results obtained for  $\text{YBa}_2\text{Cu}_3\text{O}_{7-\delta}$  related materials (Zn and Pr-substituted as well as oxygen-depleted systems) and for  $\text{La}_{2-x}\text{Sr}_x\text{CuO}_4$  are discussed.

## 1 INTRODUCTION

Historically, the isotope effect (IE) played a major role in unravelling the questions related to the origin of the effective attractive interaction between charge-carriers which leads to the superconducting state. The theoretical considerations of Fröhlich[1] and the experimental discovery of the IE of  $T_c$  in mercury[2] pointed towards the contribution of lattice dynamics to the instability of the normal state. Since then, the IE has often been considered as a measure of the contribution of phonons to the pairing mechanism. Furthermore, it is generally assumed that only those thermodynamical quantities that depend explicitly on the phonon frequencies (as  $T_c$  or the order parameter  $\Delta$  in the BCS model) display an IE.

One can show[3, 4, 5, 6, 7], however, that such understanding of the isotope effect is incomplete and leads, therefore, to confusion; this is particularly true for the high-temperature oxides. Indeed, several factors not related to the pairing mechanism can alter the value of the isotope coefficient (IC). Moreover, these factors are not necessarily related to lattice dynamics. Here we focus our attention on three such factors: magnetic impurities, the proximity effect and non-adiabatic charge-transfer as it occurs in high- $T_c$  superconductors.

In addition, we also show [6] that fundamental quantities such as the penetration depth  $\delta$  of a magnetic field also display an IE because of the three factors mentioned above. Note

that this effect occurs despite the fact that  $\delta$  does not explicitly depend on quantities related to lattice dynamics.

It results from our considerations that the value of the IC (even its absence) does not allow any *a priori* conclusion about the pairing mechanism. Nevertheless, it remains an interesting effect that enables one to determine the presence of magnetic impurities, proximity effect or non-adiabaticity in the system. The calculation of the IC and its comparison with experimental results was also used in previous works to determine the value of the Coulomb repulsion  $\mu^*$  or the relative weight of different electron-phonon coupling strengths in superconductors (see below). It can thus be used as a tool for the characterization of superconductors.

This review is mainly based on our papers[3, 4, 5, 6, 7]. We apply the theory to analyse the oxygen isotope effect of  $T_c$  in Zn and Pr-doped (YBCZnO and YPrBCO) as well as oxygen-depleted  $\text{YBa}_2\text{Cu}_3\text{O}_{7-\delta}$  (YBCO). We also review calculations of the penetration depth isotope effect. The latter superconducting property is a good example of a quantity that does not directly depend on phonon frequencies and yet can display a substantial isotopic shift [6]. In this context, we also discuss recent experimental results obtained for  $\text{La}_{2-x}\text{Sr}_x\text{CuO}_4$  (LSCO).

The structure of the paper is as follows. In section 2 we present some of the early results related to the isotope effect and show that even for conventional superconductors the relation between the isotope effect and the pairing mechanism is not simple. We also discuss the applicability of these early results to the description of high-temperature superconductors.

The remaining sections are devoted to the description of new, unconventional isotope effects. In section 3 we study the influence of magnetic impurities on the value of the isotope effect. We show that adding magnetic impurities to a superconductor can enhance the isotope coefficient  $\alpha$  of  $T_c$  and induce a temperature-dependent isotope effect of  $\delta$ . We show that both isotope effects are universal functions of  $T_c$ . That is,  $\alpha(T_c)$  and  $\beta(T_c)$  are independent of any adjustable parameter. We discuss Zn-doped  $\text{YBa}_2\text{Cu}_3\text{O}_{7-\delta}$  in this context.

Section 4 is concerned with the influence of a normal layer on the isotope effect of a superconductor. We show that due to the proximity effect, the isotope coefficient of  $T_c$  is linear in the ratio of the normal to the superconducting film thicknesses  $\rho$ . Furthermore, the proximity effect induces a temperature and  $\rho$ -dependent isotope coefficient of the penetration depth.

Section 5 reviews the concept of the non-adiabatic isotope effect introduced in Ref. [3] and further discussed in Refs. [4, 5, 6, 7]. We show that in systems as the high-temperature superconductors where charge-transfer processes between reservoir and  $\text{CuO}_2$ -planes occur via ions that display a non-adiabatic behaviour, the charge-carrier density in the planes depend on the ionic mass. This leads to the unconventional non-adiabatic contribution to the IE of  $T_c$ . It is also interesting that non-adiabaticity induces an isotopic shift of the penetration depth  $\delta$ .

In the last section (Sec. 6) we apply our theory to the oxygen isotope effect (OIE) in high-temperature superconductors of the YBCO-family. Focus is set on the oxygen isotope effect because most experimental studies have been performed on the oxygen ion which is the lightest in the  $\text{CuO}_2$  plane. The situation is less clear in the case of copper isotopic substitution where an effect has also been observed[8, 9]. This latter case will be discussed in more detail elsewhere.

We conclude the review in section 7.

## 2 THE ISOTOPE EFFECT: DISCOVERY, CONVENTIONAL VIEW

The isotope effect of superconducting critical temperature  $T_c$  is best described in terms of the isotope coefficient (IC)  $\alpha$  defined by the relation  $T_c \sim M^{-\alpha}$ , where  $M$  is the ionic mass. Under the assumption that the shift  $\Delta T_c$  induced by isotopic substitution ( $M \rightarrow M^*$ ) is small compared to  $T_c$ , one can write

$$\alpha = -\frac{M}{\Delta M} \frac{\Delta T_c}{T_c}, \quad (1)$$

where  $\Delta M = M - M^*$  is the difference between the two isotopic mass. If the superconductor is composed of different elements, one defines a *partial* isotope coefficient  $\alpha_r$  as in Eq. (1), but where  $M$  is replaced by  $M_r$ , the mass of element  $r$  that is substituted for its isotope. In addition, one defines the total isotope coefficient by

$$\alpha_{tot} = \sum_r \alpha_r = -\sum_r \frac{M_r}{\Delta M_r} \frac{\Delta T_c}{T_c}. \quad (2)$$

Besides  $T_c$  there are other quantities that display an isotope effect. In the next sections we focus on the isotope shift of the penetration depth  $\delta$ . In analogy to the IC of  $T_c$  (denoted  $\alpha$ ) we define the isotope coefficient  $\beta$  of the penetration depth by the relation

$$\beta = -\frac{M}{\Delta M} \frac{\Delta \delta}{\delta}. \quad (3)$$

One should note that there is a conventional BCS-type isotope effect of the penetration depth related to its temperature dependence  $\delta^{-2} \sim (1 - T^4/T_c^4)$ . Because  $T_c$  displays an isotope effect, the penetration depth is also shifted upon isotopic substitution. The effect becomes strong as one approaches  $T_c$ . The present article is not concerned with this trivial effect.

Let us first discuss what values of the isotope coefficients  $\alpha$  and  $\beta$  can be expected for different types of superconductors. Table 1 shows characteristic values of the isotope coefficient for different types of superconductors. Very different values of the IC have been observed (in the range from  $-2$  to  $+1$ ). One notes that some systems have a negligible coefficient, some display even an “inverse isotope coefficient” ( $\alpha < 0$ ) and some take values greater than  $0.5$ , the value predicted by Fröhlich and the BCS model (for a monoatomic system). The purpose of the next paragraphs is to describe shortly different theoretical models allowing one to understand the coefficients observed (see Table 1 and Refs. [10, 11]). We begin with the description of conventional superconductors and discuss the relevance of these models for high- $T_c$  materials. In the following sections we then introduce new considerations about the IE allowing one to give a consistent picture of the IE in high-temperature superconductors.

**Table 1.** Experimental values of the isotope coefficient of  $T_c$  (see also Refs. [11, 20]). The letters in the last column correspond to Ref. [2].

Superconductor	$\alpha$	Reference (see [2])
Hg	$0.5 \pm 0.03$	a
Tl	$0.5 \pm 0.1$	a, and [11]
Cd	$0.5 \pm 0.1$	b
Mo	$0.33 \pm 0.05$	c
Os	$0.21 \pm 0.05$	d,e
Ru	0.0	e
Zr	0.0	e
PdH(D)	-0.25	[33, 34]
U	-2	[12]
$\text{La}_{1.85}\text{Sr}_{0.15}\text{CuO}_4$	0.07	[55]
$\text{La}_{1.89}\text{Sr}_{0.11}\text{CuO}_4$ ( $^{16}\text{O} - ^{18}\text{O}$ subst.)	0.75	[55]
$\text{K}_3\text{C}_{60}$ ( $^{12}\text{C} - ^{13}\text{C}$ subst.)	0.37 or 1.4	[40]

## 2.1 Monoatomic Systems

Let us begin with the case of a monoatomic BCS-type superconductor. Substituting the atoms by an isotope affects the phonon dispersion (for a monoatomic lattice  $\Omega \sim M^{-1/2}$ , where  $\Omega$  is a characteristic phonon frequency). Thus, any quantity that depends on phonon frequencies is affected by isotopic substitution. Assuming that the electron-electron pairing interaction is mediated by phonons and neglecting the Coulomb repulsion between electrons, the BCS theory predicts that  $T_c \propto \Omega$  (see below, Eq. (4) for  $\mu^* = 0$ ). Thus, for a monoatomic system the isotope coefficient of  $T_c$  given by Eq. (1) is  $\alpha = 0.5$ .

As seen in Table 1, the IC of most monoatomic non-transition metals is approximately equal to 0.5. Many other systems, on the other hand, deviate from this value. In particular, transition metals and alloys display values that are smaller than, or equal to 0.5. PdH displays an inverse isotope effect  $\alpha_{PdH} \simeq -0.25$  [33] (there is also one report on a large inverse IC of Uranium  $\alpha_U \simeq -2$  [12]). Furthermore, high- $T_c$  materials can have values both smaller and larger than 0.5, depending on the doping.

## 2.2 The Coulomb Interaction

One of the first reasons advanced to explain the discrepancy between theory ( $\alpha = 0.5$ ) and experiment was that the BCS calculation described above did not take properly into account the Coulomb repulsion between charge-carriers. It was shown in Refs. [13, 14, 15, 16] that inclusion of Coulomb interactions leads to the introduction of the pseudo-potential  $\mu^*$  in the BCS equation for  $T_c$ :

$$T_c = 1.13\Omega \exp\left(-\frac{1}{\lambda - \mu^*}\right) \quad , \quad (4)$$

where  $\mu^*$  is the pseudo-potential given by

$$\mu^* = \frac{\mu}{1 + \mu \ln\left(\frac{E_F}{\Omega}\right)} \quad . \quad (5)$$

$\mu$  is the Coulomb potential and  $E_F$  is the Fermi energy. One notes that  $\Omega$  is present in  $\mu^*$  and thus in the exponent of Eq. (4). The value of  $\alpha$  can thus be substantially decreased from 0.5. Indeed, from Eq. (1) and (4) one obtains

$$\alpha = \frac{1}{2} \left\{ 1 - \left( \frac{\mu^*}{\lambda - \mu^*} \right)^2 \right\} . \quad (6)$$

The isotope coefficient is shown as a function of  $\lambda$  for different values of  $\mu^*$  in Fig. 1. Naturally, only the case  $\lambda > \mu^*$  is relevant, since superconductivity is otherwise suppressed.

The effect of Coulomb interactions can be included in a similar way in the strong-coupling Eliashberg theory. Using the formula derived by McMillan [17]:

$$T_c = \frac{\Omega}{1.2} \exp \left( -\frac{1.04(1+\lambda)}{\lambda - \tilde{\mu}} \right), \quad (7)$$

with  $\tilde{\mu} \equiv (1 + 0.62\lambda)\mu^*$  and  $\mu^*$  is given by Eq. (5), one obtains the following result for the isotope coefficient:

$$\alpha = \frac{1}{2} \left\{ 1 - \frac{1.04(1+\lambda)\tilde{\mu}\mu^*}{[\lambda - \tilde{\mu}]^2} \right\} . \quad (8)$$

A similar result has also been derived in Ref. [10]. Fig. 1 shows the dependence described by Eq. (8) and allows one to compare the weak and strong-coupling cases, that is, Eqs. (6) and (8).

An expression for  $T_c$  that is valid over the whole range of coupling strengths (from weak to very strong couplings) has been derived by one of the authors in Ref. [18]:

$$T_c = \frac{0.25\Omega}{\sqrt{e^{2/\lambda_{eff}} - 1}} \quad (9)$$

with

$$\lambda_{eff} = \frac{\lambda - \mu^*}{1 + 2\mu^* + \lambda\mu^*t(\lambda)} , \quad (10)$$

and  $t(\lambda) \simeq 1.5 \exp(-0.28\lambda)$  [18]. As usual, the parameter  $\mu^*$  is given by Eq. (5). The isotope coefficient resulting from Eq. (1), (9) and (10) reads

$$\alpha = \frac{1}{2} \left\{ 1 - \frac{\mu^{*2}}{\lambda_{eff} \left( 1 - e^{-2/\lambda_{eff}} \right)} \left[ \frac{1}{\lambda - \mu^*} + \frac{2 + \lambda t(\lambda)}{3 + \lambda t(\lambda)} \right] \right\} . \quad (11)$$

This isotope coefficient is also displayed in Fig. 1 for two values of the parameter  $\mu^*$ . Note that for all models, because of the presence of  $\mu^*$  the isotope coefficient of  $T_c$  is lowered with respect to the BCS value for  $\alpha = 0.5$ . One recovers the BCS result asymptotically at large  $\lambda$  (or  $T_c/\Omega$ ). Only Eq. (11), however, is valid in the strong coupling limit ( $\lambda > 1$ ).

An interesting general feature of the results presented above is that the strongest deviation from the BCS monoatomic value 0.5 occurs when  $\mu^*$  (or  $\tilde{\mu}$ ) is of the order of  $\lambda$  (see Eqs. (6), (8) or (11)). Thus, excluding anharmonic or band-structure effects, a *small* isotope coefficient is correlated to a *low*  $T_c$ . This is indeed observed in most conventional superconductors. In certain cases one even obtains a *negative* (also called *inverse*) isotope coefficient ( $\alpha < 0$ ). For realistic values of the parameters,  $T_c$  should not exceed  $T_c \sim 1\text{K}$  for this inverse effect to be present. Several systems display this inverse isotope effect, among them PdH (where H is

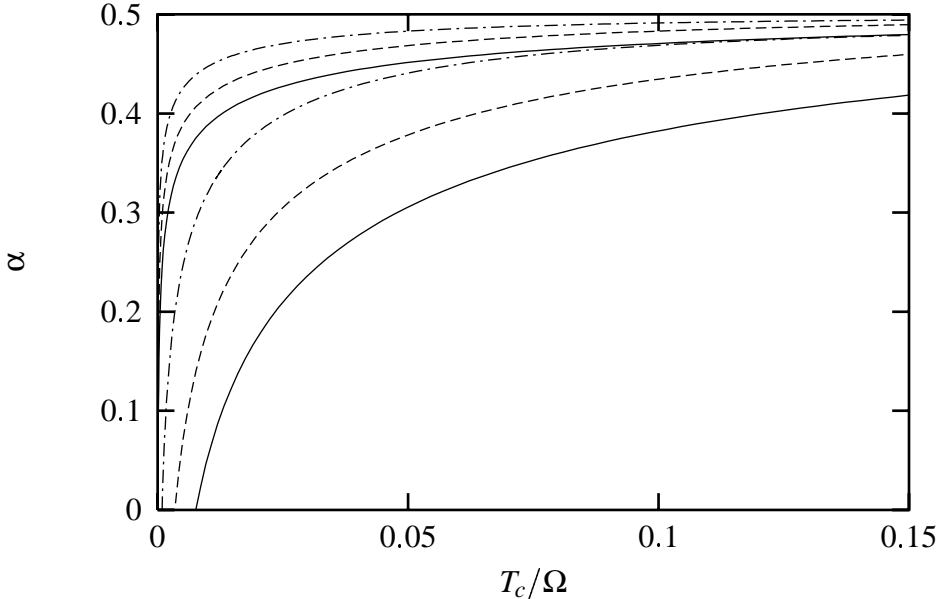


**Figure 1.** Isotope coefficient  $\alpha$  as a function of  $T_c/\Omega$  (i.e.  $\lambda$ ) for different values of  $\mu^*$ . Solid lines from Eq. (6), dashed lines from Eq. (8) and dash-dotted lines from Eq. (11). For each type of line, the upper curve corresponds to  $\mu^* = 0.1$  and the lower to  $\mu^* = 0.2$ .

replaced by its isotope D) [33, 34] and Uranium (where  $^{235}\text{U}$  is replaced by  $^{238}\text{U}$ ) [12]. We discuss this case below (sec. 2.3).

The situation encountered in high-temperature superconductors is very unusual. Indeed, one observes that the isotope coefficient has a *minimum* value at optimal doping (*highest*  $T_c$ ). The explanation of a small  $\alpha$  for oxygen substitution coinciding with a high  $T_c$  is likely to be related to the contribution of the oxygen modes to the pairing.

The main conclusion of this section is that the Coulomb interaction and its logarithmic weakening leads to the deviation of the isotope coefficient from the value  $\alpha = 0.5$  and to the non-universality of  $\alpha$ .

### 2.3 Band Structure Effects; Transition Metals

Up to now we have only considered the effect on  $T_c$  induced by the isotopic shift of phonon frequencies. Furthermore, we have considered the case where the phonon frequency appears explicitly in the expression for  $T_c$  (as prefactor and in  $\mu^*$ ; see Eqs. (4), (7) and (9)). Band structure effects have first been considered to explain the discrepancies observed between the results following from the strong-coupling McMillan equation (Eq. (7)) and the IC measured in transition metals. Several other generalizations of the basic model have been considered, especially in the context of high-temperature superconductors.

Let us first describe the situation encountered in transition metals. As has been shown in Refs. [15, 16], the two-square model for which (5) is derived leads to values of the IC that are only 10 – 30% lower than 0.5. However, the deviation is much stronger for some transition metals, leading even to a vanishing coefficient for Ruthenium. As shown in Ref. [19] it is necessary to take into account the band structure of transition metals. The presence of a “metallic”  $s$ -band and a narrow  $d$ -band, and the associated peaked structure of the electronic density of states (DOS) has an impact on the value of  $\mu^*$ . Furthermore,  $E_F$  is much smaller in transition metals than in non-transition metals and leads thus to a smaller effective screening of the Coulomb interaction. These facts have been included in Ref. [19] by modifying the two square-well model used to derive Eq. (5). The values obtained from the modified expression of  $\alpha$  (see Eq. (9) in Ref. [19]) are in good semi-quantitative agreement with the experimental

results.

One should add that the two-band structure is important even in dirty transition-metal superconductors, although the superconducting state is characterized by only one gap in this case (see Ref. [11] for further discussions on transition metals).

The example of transition metals shows that a quantitative description of the IC requires, among other things, a precise knowledge of the band structure. This has also been suggested in Ref. [12, 20] to explain the large inverse isotope effect observed in Uranium. In this context, it would be interesting to determine the uranium isotope effect in heavy-fermion systems (one should note, however, that there is only one report of the isotope effect in uranium[12]).

Another effect of the band structure arises if one assumes that the electronic density of states varies strongly on a scale given by  $\Omega$ , the BCS energy cutoff (e.g., in the presence of a van Hove singularity). To obtain the BCS expression (4) we assumed that the electronic density of states (DOS) is constant in the energy interval  $[-\Omega, \Omega]$  around the Fermi energy.  $\lambda$  is then given by  $N(E_F)V$ , where  $N$  is the DOS at the Fermi level and  $V$  is the attractive part of the electron-electron effective interaction. In a more general case, however, one has to consider the energy dependence of the DOS. Though a purely electronic parameter, the energy dependence of the DOS appears to influence the isotope effect[21]. One can understand this effect qualitatively within a crude extension of the BCS model. Instead of taking the DOS at the Fermi level, one replaces  $N(E_F)$  by  $\langle N(\epsilon) \rangle_\Omega$ , the average value of the DOS  $N(\epsilon)$  over the interval  $[-\Omega, \Omega]$  around  $E_F$ . Obviously, this average depends on the cutoff energy  $\Omega$  of the pairing interaction. Isotopic substitution modifies  $\Omega$  which affects  $\langle N(\epsilon) \rangle_\Omega$ , and thus  $\lambda = \langle N \rangle_\Omega V$  and  $T_c$ .

A more general analysis of this effect within Eliashberg's theory was given in Ref. [21]. They find that whereas the IC can reach values above 0.5, its minimal value obtained for reasonable choices of the parameters never reaches the small values ( $\sim 0.02$ ) found in optimally doped high- $T_c$  compounds. However, more recent studies of the influence of van Hove singularities on the isotope coefficient show that such small values can be obtained, because in this scenario the cutoff energy for the effective interaction between charge-carriers is given by  $\min(E_F - E_{vH}; \Omega)$  (where  $E_{vH}$  is the energy of the van Hove singularity and  $\Omega$  is a characteristic phonon energy) [22, 23, 24]. If the cutoff energy is given by  $E_F - E_{vH}$  and is thus electronic in origin,  $T_c$  displays no shift upon isotopic substitution. Taking into account the Coulomb repulsion it has been shown[24] that one can even obtain a negative IC.

Another way to extend the results presented earlier is to consider an anisotropic Eliashberg coupling function  $\alpha^2 F(\mathbf{q}, \omega)$ . Generally it is assumed that the system is isotropic and the coupling function can be averaged over the Fermi surface, leading to a  $\mathbf{q}$ -independent Eliashberg function. If the system is strongly anisotropic (as is the case of high- $T_c$  superconductors), the average may not lead to an accurate description of the situation. The isotope effect has been studied for different  $\mathbf{q}$ -dependent form factors entering  $\alpha^2 F$  in Ref. [25]. They show that a small isotope coefficient as observed in  $\text{YBa}_2\text{Cu}_3\text{O}_{7-\delta}$  can be obtained for anisotropic systems. Nevertheless, to obtain high critical temperatures at the same time, they are forced to introduce another, electronic pairing mechanism. Such a situation is further discussed below (see Sec. 2.6).

Note that the theories presented in this section give only a qualitative picture of the situation encountered in high-temperature superconductors and do presently not account for the isotope effect observed in various systems (see also Refs. [21, 26]).

## 2.4 Polyatomic Systems

Until now we focused mainly on the study of monoatomic systems in which the attractive interaction leading to the formation of pairs is mediated by phonons. All previous effects are naturally also encountered in polyatomic systems. However, the presence of two or more elements in the composition of a superconductor has several direct consequences for the isotope effect that we summarize in the following. The first consequence of a polyatomic system is that the characteristic frequency  $\Omega$  which determines the value of  $T_c$  depends on the mass of the different ions involved  $\Omega = \Omega(M_1, M_2, \dots)$ . Obviously, the dependence  $\Omega \sim M_r^{-\alpha_r}$  for element  $r = 1, 2, \dots$  must not be equal to  $\alpha_r = 0.5$ . It is thus not surprising if the partial isotope coefficient (obtained by substituting one type of ions for its isotope; see Eq. (3)) differs from the textbook value 0.5.

Let us consider the example of a cubic lattice with alternating masses  $M_1$  and  $M_2$ [27, 28]. The acoustic and optical branches can be calculated analytically[27]. From this one obtains the following partial isotope coefficients:

$$\alpha_1 = \frac{1}{2\Omega^2 M_1} \left\{ \bar{K} \pm \frac{\bar{K}^2 M_{12}^- + 2\bar{K}_L/M_2}{(\Omega \mp \bar{K}M_{12}^+)} \right\} , \quad (12)$$

$$\alpha_2 = \frac{1}{2\Omega^2 M_2} \left\{ \bar{K} \pm \frac{-\bar{K}^2 M_{12}^- + 2\bar{K}_L/M_1}{(\Omega \mp \bar{K}M_{12}^+)} \right\} , \quad (13)$$

where  $M_{12}^- = M_1^{-1} - M_2^{-1}$ ,  $M_{12}^+ = M_1^{-1} + M_2^{-1}$ . The upper sign stands for the Debye frequency and the lower sign has to be considered when the characteristic frequency is given by the optical phonon.  $\bar{K} = \sum_{x,y,z} K_i$  is the sum of the force constants and  $\bar{K}_L = \sum_{x,y,z} K_i \cos(qL)$  ( $q = 0$  for the optical branch and  $q = \pi/L$  for acoustic mode;  $L$  is the lattice constant). One notes that the total isotope coefficient is given by  $\alpha_{tot} = \alpha_1 + \alpha_2 = 0.5$  whether one takes the acoustical or the optical phonon as the characteristic energy for the determination of  $T_c$ .

Given the previous result, one can ask if there exists a maximal value of the IC. It is often stated in the literature that 0.5 is the maximal value that the isotope coefficient can reach within a harmonic phonon, and electron-phonon induced pairing model. Although to the knowledge of the authors none of the systems studied so far seems to contradict this assertion, one should note that there is no proof of this statement. It was shown in Ref. [29] that for a polyatomic system  $\alpha_{tot} \equiv \sum_r \alpha_r = 0.5$  (defined in Eq. (2)) if one assumes that  $\mu^* = 0$  and all masses of the unit cell are subject to *the same* isotopic shift (i.e.,  $\Delta M_r/M_r$  takes the same constant value for each element  $r$  of the system, see Eq. (2)). These assumptions hold approximately for certain systems as, e.g., the Chevrel-phase  $\text{Mo}_6\text{Se}_8$  material[29], but are certainly not valid for example in high-temperature superconductors. It is thus not clear if the *total* isotope coefficient, Eq. (2), is indeed always 0.5. The general proof of such a statement requires the knowledge of the polarization vectors and their derivatives with respect to the isotopic masses, both of which have to be calculated for each specific system studied.

Another important remark concerns the value of the (very small) IC for optimally doped high- $T_c$  superconductors. Experimentally one measures generally the partial oxygen isotope effect (in some cases also the Cu and Ba IE). Since the unit cell of a high-temperature superconductor contains many different atoms, one expects values of the partial IC that are significantly smaller than 0.5. A crude estimate can be given by observing that under the assumption of a same contribution of each atom to the isotope coefficient (which is certainly not the case as mentioned above) the value of the isotope effect for oxygen in YBCO would be  $\alpha \approx 0.5/N \approx 0.04$ , where  $N$  is the number of atoms per unit cells ( $N = 13$  in the case of YBCO). Since there are 6 – 7 oxygen atoms in the unit cell, one should multiply  $\alpha_{ox}$  by this number.

If, in addition to the multiaatomic structure of the system, one takes into account the effect of Coulomb interactions and/or the fact that the charge-carriers may strongly couple to certain phonons only one can obtain values of the order observed in high-temperature oxides. The second possibility has for example been studied in the context of the Chevrel-phase compound  $\text{Mo}_6\text{Se}_8$ [29] or organic superconductors[30]. It has also been studied for high- $T_c$  superconductors in Ref. [31, 32]. They conclude that the oxygen isotope effect can be well described for reasonable parameters in the case of  $\text{La}_{2-x}\text{Sr}_x\text{CuO}_4$ , but that unphysical values of the coupling have to be considered to describe the partial oxygen isotope effect of  $\text{YBa}_2\text{Cu}_3\text{O}_{7-\delta}$ . A careful study of the effect of Coulomb interactions on the IE of high- $T_c$  superconductors has not been done yet.

On thus concludes from the previous considerations that it is not impossible to explain the small values of the IC observed in conjunction with high  $T_c$ 's in high-temperature materials, if one considers the combined effect of a polyatomic system, the Coulomb interaction and the band structure.

## 2.5 Anharmonicity

Anharmonic effects play an important role in materials such as PdH(D)[33, 34],  $\text{Mo}_6\text{Se}_8$ [29] or, according to some theories[26, 35, 36, 37], in high-temperature superconductors. Among other consequences the presence of anharmonicities affects the value of the isotope coefficient. We present here two different aspects of the anharmonic isotope effect: anharmonicity of the characteristic phonon mode (for PdH) and volume effects (for Molybdenum).

Quantities that are independent of ionic masses in the harmonic approximation, can become mass dependent in the presence of anharmonicity. We mention three such properties that are of interest for the isotope effect in superconductors: the lattice force constants  $K_i$ [34], the unit-cell volume [38, 39] and the electron-phonon coupling function  $\lambda$ [26, 35]. In the first case, it was shown that the account of Coulomb interactions alone (see above) cannot explain the inverse ( $\alpha < 0$ ) hydrogen isotope effect observed in PdH (see Table 1). On the other hand, a change of 20% of the lattice force constants when replacing H for Deuterium (D) in PdH was inferred from neutron-scattering data[34]. This results from large zero-point motion of H as compared to D. Taking this fact into account in the Eliashberg formalism allows one to obtain quantitative agreement with the experiment[34].

Another effect due to the presence of anharmonicity is the isotopic volume effect[38, 39]. This effect was discussed in the context of Molybdenum and is related to the difference in zero-point motion of the two isotopes. In such a system one can write the IC as  $\alpha = \alpha_{BCS} + \alpha_{vol}$  with

$$\alpha_{vol} = B \frac{M}{\Delta M} \frac{\Delta V}{V} \frac{\Delta T_c}{\Delta P} , \quad (14)$$

where  $B = -V \partial P / \partial V$  is the bulk modulus,  $P$  is the pressure and  $\Delta V = V^* - V$  is the volume difference induced by isotopic substitution. In the case of Molybdenum the volume isotope effect amounts to  $\alpha_{vol} \approx 0.09$  and accounts for  $\sim 27\%$  of the total isotope coefficient, which is not a negligible effect.

The presence of a volume isotope effect has also been suggested in the case of PdH,  $\text{C}_{60}$  materials as well as in Pb[38].

The other major effect of anharmonicity is the appearance of an ionic-mass dependent electron-phonon coupling function  $\lambda$ [26, 35, 42]. In this case not only the prefactor  $\Omega$  of Eq. (4), but also the exponent depends on ionic masses. As stressed earlier in the context of band structure effects, this fact can lead to a strong deviation from  $\alpha_{BCS} = 0.5$ , even for monoatomic systems. An explicit expression for the motion of the oxygen in a simple

double-well potential was obtained in Ref. [35] for high- $T_c$  superconductors. The model was extended further in Refs. [35]b and [26] and it was shown that the isotope coefficient can be much smaller than 0.5 with moderate values of the coupling constant or exceed 0.5 for (very) strong couplings (the function  $\alpha(\lambda)$  goes through a minimum at  $\lambda \sim 1$ ; see Ref. [35]). Regarding high- $T_c$  superconductors, the anharmonic model could explain qualitatively the behaviour of the isotope coefficient if one considers the fact that the coupling function  $\lambda$  also depends on doping (see Ref. [43] for this dependency). Assuming that these systems are strong-coupling superconductors, and that the coupling decreases upon doping, one can describe qualitatively the behaviour of  $\alpha(T_c)$  for underdoped systems. However, it is difficult to obtain quantitative agreement especially in the optimally doped and strongly underdoped regime. In the first case the coupling has to be intermediate to obtain small  $\alpha$ 's but then  $T_c$  is also small. In the second, strongly underdoped case, the IC can exceed 0.5, but the coupling has to be very strong. One way to solve this problem is to assume that the superconducting pairing is mediated by an additional, non-phononic channel (see Ref. [42] and below).

The influence of anharmonicity on the electron-phonon coupling  $\lambda$  and on the hopping parameter (for a tight-binding type of lattice) has also been considered in the context of  $^{12}\text{C} \leftrightarrow ^{13}\text{C}$  isotope substitution in  $A_3\text{C}_{60}$  materials ( $A = \text{Na}, \text{Ru}$ ; see, e.g., Ref. [40] and references therein). Experimentally the isotope coefficient was shown to vary between 0.37 to 1.4, depending on the isotopic substitution process (in the first case each  $\text{C}_{60}$  molecule contains an equal amount of  $^{12}\text{C}$  and  $^{13}\text{C}$  isotopes whereas in the second case the system contains  $\text{C}_{60}$ -molecules that are composed of either pure  $^{12}\text{C}$  or pure  $^{13}\text{C}$  atoms) [40].

## 2.6 Non-Phonon and Mixed Mechanisms

The superconducting transition can also be caused by a non-phonon mechanism. Historically, the introduction of the electronic mechanisms [41] started the race for higher  $T_c$ 's. The pairing can be provided by the exchange of excitations such as excitons, plasmons, magnons etc... (see, e.g., Ref. [28]). In general, one can have a combined mechanism. An electronic channel can provide for an additional contribution to the pairing, as is the case, e.g., in a phonon-plasmon mechanism [44]. In the context of the isotope effect, the mixed mechanism may provide for an explanation for the unusual occurrence of high  $T_c$ 's and small isotope coefficients  $\alpha$  (see above).

Let us initially consider the case where only electronic excitations mediate the pairing interaction and the Eliashberg function  $\alpha^2 F$  can be approximated by a single peak at energy  $\Omega_e$ , the characteristic electronic energy. The theory considered in weak coupling yields then a relation of the form  $T_c \simeq \Omega_e e^{-1/\lambda}$ . For an electronic mechanism  $\Omega_e$  is independent of the ionic mass. Therefore, the isotope coefficient of  $T_c$  vanishes for such cases.

If, on the other hand, the superconducting state is due to the combination of phonon and a high-energy excitations (as, e.g., plasmons [44]) then one has to include both excitations in  $\alpha^2 F$ . In this case, the simplest model considers an Eliashberg function composed of two peaks, one at low energies ( $\Omega_0$ ) for the phonons and one at high energies ( $\Omega_1$ ) for the electronic mechanism. For such a model, one obtains the following expression for  $T_c$ [45]:

$$T_c = 1.14 \Omega_0^{f_0} \Omega_1^{f_1} \exp \left( -\frac{h(\rho_i, \Omega_i)}{\rho_0 + \rho_1} \right) \quad (15)$$

where  $h$  is a slow varying function of  $\rho_i$  and  $\Omega_i$ ,  $f_i = \rho_i / (\rho_0 + \rho_1)$  and  $\rho_i = \lambda_i / (1 + \lambda_0 + \lambda_1)$  ( $i = 1, 2$ ). In weak coupling,  $h \approx 1$  and the exponent is independent of the ionic masses. The resulting isotope coefficient for this mixed mechanism takes then the form:

$$\alpha = \frac{f_0}{2} = \frac{1}{2} \left\{ 1 - \frac{\lambda_1}{\lambda_0 + \lambda_1} \right\} \quad . \quad (16)$$

If only the phonon mechanism is active  $\lambda_1 = 0$  and one recovers the BCS value 0.5. Otherwise, the presence of the non-phononic mechanism reduces the value of the isotope coefficient, while enhancing  $T_c$ . For  $\lambda_0 \ll \lambda_1$  one has  $\alpha \approx 0$ . A joint mechanism would thus allow one to explain the small values of the IC for optimally doped high- $T_c$  superconductors since the coupling to non-phononic degrees of freedom would provide for high  $T_c$ 's while it would reduce, together with the Coulomb repulsive term, the value of the IC.

Another way to include non-phononic contributions to the pairing mechanism, is to consider a negative effective Coulomb term  $\mu^*$  in the Eliashberg theory[28, 46, 31]. The pseudo-potential  $\mu^*$  can thus be seen as an effective attractive pairing potential contribution and thus supports superconductivity. Such a negative  $\mu^*$  is for example obtained in the plasmon model [44, 28, 46]. One notes that the small values of the partial isotope coefficient in optimally doped high- $T_c$  materials can easily be explained within such a model.

Several other non-phononic as well as combined mechanisms have been proposed [31, 42, 47, 48] that also lead to a reduction of the isotope effect. We refer to the literature for the details.

## 2.7 Isotope Effect of Properties other than $T_c$

All previous considerations were concerned with the isotope effect of the superconducting critical temperature  $T_c$ . One can ask if there are other properties displaying an isotope effect in conventional superconductors. Naturally, every quantity depending directly on phonon frequencies will display such an effect. Let us consider here a property that will be studied further in the next sections, namely the penetration depth of a magnetic field  $\delta$ . In the weak-coupling London limit the penetration depth is given by the well-known relation

$$\delta^2 = \frac{mc^2}{4\pi n_s e^2} = \frac{mc^2}{4\pi n \varphi(T/T_c) e^2} . \quad (17)$$

where  $m$  is the effective mass.  $n_s$  is the superconducting density of charge carriers, related to the normal density  $n$  through  $n_s = n\varphi(T/T_c)$ . The function  $\varphi(T/T_c)$  is a universal function of  $T/T_c$ . For example,  $\varphi \simeq 1 - (T/T_c)^4$  near  $T_c$ , whereas  $\varphi \simeq 1$  near  $T = 0$  (in the absence of magnetic impurities; their influence is discussed in section 3).

Eq. (17) does not depend explicitly on phonon frequencies. Nevertheless, it can display an isotopic dependence through  $T_c$ . In fact, this dependency is common to all superconducting properties within the BCS theory. Indeed, all major quantities such as heat capacity, penetration depth, critical field, thermal conductivity etc... can be expressed as universal functions of  $T_c$ . As a result, all these quantities display a trivial isotopic shift, caused by the isotopic shift in  $T_c$ . The value of the shift is growing as one approaches  $T_c$ . Furthermore, the shift vanishes for  $T \rightarrow 0$ . As will be shown in section 3 and following the situation is very different in high-temperature superconductors and manganites. For example, the influence of non-adiabaticity on charge-transfer processes results in an unconventional ionic mass dependence of the charge-carrier concentration  $n = n(M)$ , which, according to Eq. (17), leads to a new isotope effect (see sec. 5).

So far, we have presented various theories explaining the deviation of the measured isotope coefficient in conventional superconductors from the value  $\alpha = 0.5$  derived within the BCS model. The remainder of this review is devoted to the study of three factors that are not related to the pairing interaction but affect the isotope coefficient: magnetic impurities, proximity contacts, and non-adiabatic charge-transfer processes. We show that they can strongly modify the value of the isotope coefficient and can even induce an isotopic shift of superconducting properties such as the penetration depth  $\delta$ . In the last part of this review, we then

apply the theory to the case of the oxygen isotopic substitution in high-temperature superconductors.

### 3 MAGNETIC IMPURITIES AND THE ISOTOPE EFFECT

The presence of magnetic impurities strongly affects various properties of a superconductor. It has been shown[49, 50] that because of magnetic impurity spin-flip scattering processes, Cooper pairs are broken and thus removed from the superconducting condensate. Several properties are affected by the pair-breaking effect. Magnetic scattering leads to a decrease of the critical temperature  $T_c$ , the energy gap, the jump in the specific heat at  $T_c$ , etc... At some critical impurity concentration  $n_M = n_{M,cr}$  superconductivity is totally suppressed. Moreover, there exists an impurity concentration  $n_M = n_{M,g} < n_{M,cr}$  (for conventional superconductors  $n_{M,g} = 0.9n_{M,cr}$ , see Ref. [49, 50]) beyond which the superconducting state is gapless. Pair-breaking also leads to an increase of the penetration depth  $\delta$ . We show in the following sections that the presence of magnetic impurities leads to a change of the isotope coefficient of  $T_c$  and  $\delta$ .

#### 3.1 The Critical Temperature

The change of  $T_c$  induced by magnetic impurities is described in the weak-coupling regime by the Abrikosov-Gor'kov equation[49]:

$$\ln\left(\frac{T_{c0}}{T_c}\right) = \psi\left(\frac{1}{2} + \gamma_s\right) - \psi\left(\frac{1}{2}\right) \quad , \quad (18)$$

where  $\gamma_s = \Gamma_s/2\pi T_c$  and  $T_c$  ( $T_{c0}$ ) is the superconducting critical temperature in the presence (absence) of magnetic impurities.  $\Gamma_s = \tilde{\Gamma}_s n_M$  is the spin-flip scattering amplitude and is proportional to the magnetic impurity concentration  $n_M$  ( $\tilde{\Gamma}_s$  is a constant).

It is easy to derive a relation between the isotope coefficient  $\alpha_0$  in the absence of magnetic impurities [ $\alpha_0 = -(M/\Delta M)(\Delta T_{c0}/T_{c0})$ , Eq. (1)] and its value in the presence of magnetic impurities [ $\alpha = -(M/\Delta M)(\Delta T_c/T_c)$ ]. From Eqs. (1) and (18) one obtains[51, 4, 5, 52]:

$$\alpha_m = \frac{\alpha_0}{1 - \psi'(\gamma_s + 1/2)\gamma_s} \quad , \quad (19)$$

where  $\psi'$  is the derivative of the psi function and is a positive monotonous decreasing function of  $\gamma_s$ . The fact that  $\alpha_0$  and  $\alpha$  are not identical relies on the essential feature that the relation between  $T_{c0}$  and  $T_c$  (Eq. (18)) is non-linear. It is interesting to note that magnetic scattering decreases  $T_c$  (reduction of the condensate) but *increases* the value of the IC ( $\alpha_m > \alpha_0$ ; see Eq. (19)).

An important consequence of Eqs. (18) and (19) is that one can write the IC as a universal function  $\alpha(T_c)$ . This relation does not contain any adjustable parameter, but depends solely on the measurable quantities  $\alpha_0$  and  $T_c$ . The universal curve is shown in Fig. 2. Note also that  $\alpha_m$  can, in principle, exceed the value  $\alpha_{BCS} = 0.5$ . Thus, the observation of large values of  $\alpha$  are not necessarily related to the pairing mechanism.

#### 3.2 Zn-doped YBa<sub>2</sub>Cu<sub>3</sub>O<sub>7-δ</sub>

Zn substitution for Cu in the CuO<sub>2</sub> planes of YBCO has attracted a lot of interest, since it leads to a drastic decrease in  $T_c$  [53] and a strong increase of the penetration depth [54]

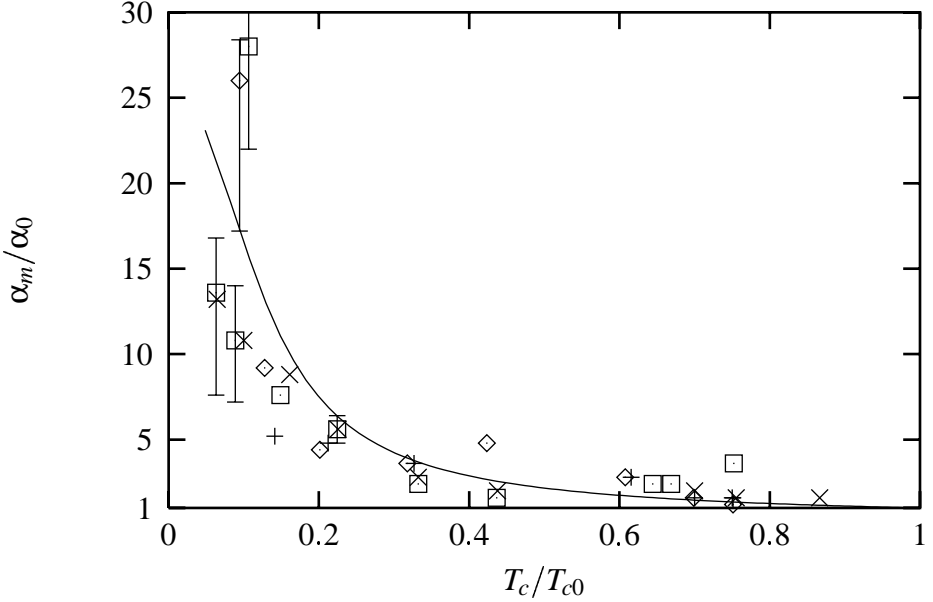


**Figure 2.** Isotope coefficient of  $T_c$  in the presence of magnetic impurities. Solid line: Universal dependence  $\alpha(T_c)$  (normalized to  $\alpha_0$ ; see Ref. [4]); Points: Isotope effect for  $\text{YBa}_2(\text{Cu}_{1-x}\text{Zn}_x)_3\text{O}_7$  obtained with various experimental techniques and normalized to  $\alpha_0 = 0.025$  (from Ref. [56, 4]).

(superconductivity is destroyed with  $\sim 10\%$  of Zn). In addition, this decrease of  $T_c$  is accompanied by an increase of the isotope coefficient (see Ref. [53, 56] and Fig. 2). We think that the peculiar behaviour of Zn doping is related to the pair-breaking effect. It has been established by several methods (see Refs. [53, 54]) that Zn substitution leads to the formation of local magnetic moments ( $\sim 0.63\mu_B/\text{Zn}$ , where  $\mu_B$  is the Bohr magneton) in the vicinity of Zn.

Fig. 2 displays the experimental results obtained for the oxygen isotope coefficient of Zn-doped YBCO[56, 4] (normalized to  $\alpha_0 \simeq 0.025$ [57]). One can see from this figure that the agreement between the theoretical dependence  $\alpha(T_c)$  and the experiment is very good. Note that the uncertainty in the data is growing as  $T_c \rightarrow 0$  (see Ref. [56]).

### 3.3 The Penetration Depth

The isotope effect of the penetration depth is more complicated than the isotope effect of  $T_c$ , since it appears to be temperature dependent. Here we present the main results near  $T_c$  and at  $T = 0$  and refer the reader to Ref. [5, 6] for details. Near  $T_c$ , the penetration depth is given in second order of the superconducting order parameter  $\Delta \equiv \Delta(T, \Gamma_s)$  by[50]:

$$\delta^{-2} = \sigma \frac{\Delta^2}{T_c} \zeta(2, \gamma_s + \frac{1}{2}) \quad , \quad (20)$$

where  $\sigma = 4\sigma_N/c$  ( $\sigma_N$  is the normal state conductivity),  $\zeta(z, q) = \sum_{n \geq 0} 1/(n+q)^z$  and  $\gamma_s$  was defined in Eq. (18). One can calculate the isotope effect from Eqs. (3), (20) and the analytical expression for  $\Delta$  near  $T_c$  (see Refs. [50, 5]):

$$\Delta^2 = 2\Gamma_s^2(1-\tau) \frac{1 - \bar{\zeta}_2 + (1-\tau) [\frac{1}{2} - \bar{\zeta}_2 + \bar{\zeta}_3]}{\bar{\zeta}_3 - \bar{\zeta}_4} \equiv 2\Gamma_s^2 \frac{N_1}{D_1} \quad (21)$$

with  $\bar{\zeta}_z = \gamma_s^{-1} \zeta(z, \gamma_s + 1/2)$ ,  $z = 1, 2, \dots$  and  $\tau = T/T_c$ .

As mentioned in Sec. 2,  $\delta$  experiences a trivial BCS isotope effect near  $T_c$ . Since we are only interested in the unconventional IE resulting from the presence of magnetic impurities, we subtract the BCS isotope effect by calculating the isotope coefficient  $\beta_m$  of

$\delta(T, \Gamma_s)/\delta(T, 0)$ . Near  $T_c$  this coefficient can be written as  $\tilde{\beta}_m = \beta_m - \beta_0$ , where  $\beta_m$  ( $\beta_0$ ) is the isotope coefficient of  $\delta$  in the presence (absence) of magnetic impurities. One can show[6] that (near  $T_c$ )  $\tilde{\beta}_m$  can be rewritten in the form:

$$\tilde{\beta}_m = (R_1 - R_0)\alpha_m \quad , \quad (22)$$

where

$$R_1 = -\frac{1}{2}f_1 = -\frac{1}{2}\left(\frac{N_2}{N_1} - \frac{D_2}{D_1} + 2\frac{\bar{\zeta}_3}{\bar{\zeta}_2} - 1\right) \quad , \quad (23)$$

$$R_0 = -\frac{1}{2}\frac{\alpha_0}{\alpha_m}f_0 = -\frac{1}{2}[1 - \psi'(\gamma_s + 1/2)\gamma_s]f_0 \quad , \quad (24)$$

and  $f_0 = (3 - \tau^2)/(1 - \tau)(3 - \tau)$ . The functions  $N_1, D_1$  are defined in Eq. (21) and

$$\begin{aligned} N_2 &= 3(1 - \tau)^2 [\bar{\zeta}_2 - 2\bar{\zeta}_3 + \bar{\zeta}_4] + \tau(2 - \tau) - \bar{\zeta}_2 \\ D_2 &= 2(3\bar{\zeta}_4 - \bar{\zeta}_3 - 2\bar{\zeta}_5) \end{aligned} .$$

This relation is valid near  $T_c$  (where  $\Delta$  is small) and for impurity concentrations such that  $\Delta T_c/T_c \ll 1$ .

One notes first that the isotope coefficient of  $\delta$  is proportional to the IC of  $T_c$ . As for the isotope coefficient of  $T_c$  (Eq. (19)) all quantities can either be obtained from experiment (e.g.,  $\alpha_0$ ,  $T_{c0}$  and  $T_c$ ) or calculated self-consistently using Eqs. (18) and (19). There is thus no free parameter in the determination of  $\tilde{\beta}_m$ . Fig. 3 displays the IC  $\tilde{\beta}_m$  (normalized to  $\alpha_0$ )

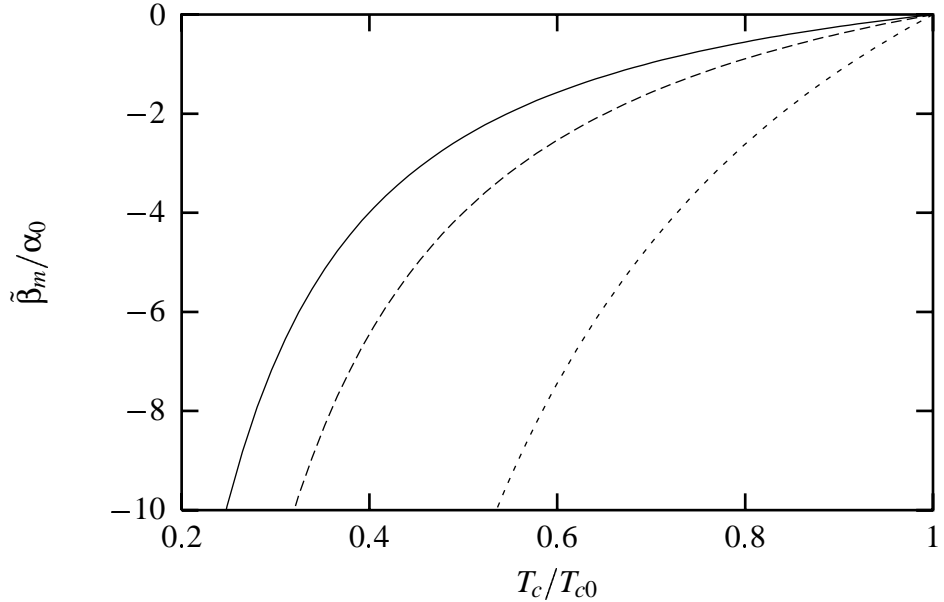


**Figure 3.** Isotope coefficient  $\tilde{\beta}_m$  near  $T_c$  (normalized to  $\alpha_0$ ) as a function of  $T_c$  (i.e. of magnetic impurity concentration) for  $T_c/T_{c0} = 0.75$  (solid line), 0.85 (dashed) and 0.95 (dotted). Multiplying by  $\alpha_0 = 0.025$  gives the IC expected for  $\text{YBa}_2(\text{Cu}_{1-x}\text{Zn}_x)_3\text{O}_{7-\delta}$ .

as a function of  $T_c$  (i.e. on the concentration  $n_M$ ) for fixed values of the temperature. Setting  $\alpha_0 = 0.025$ , one obtains the relation  $\alpha(T_c)$  expected for YBCZnO. It would be interesting to measure the isotope effect of  $\delta$  near  $T_c$  in this system, to verify our predictions.

An interesting property of Eq. (22) that is shown in Fig. 3 is the fact that the isotope coefficient of  $\delta$  is temperature dependent; an unusual feature in the context of the isotope effect. We will see in Sec. 4 that a temperature dependent IC is also observed for a proximity system.

As can be seen by comparing Figs. 2 and 3, the qualitative behaviour of  $\tilde{\beta}_m(T_c)$  is similar to  $\alpha_m(T_c)$  [Eq. (19) with  $\alpha_0 = \alpha_{ph}$ ] but with opposite sign. Furthermore, in the absence of magnetic impurities one has  $\tilde{\beta}_m = 0$ , whereas  $\alpha_m(T_c) = \alpha_{ph}$ .

Note finally, that since  $R_1 - R_0 < 0$ , the IC of the penetration depth is always negative when magnetic impurities are added to the system. This conclusion might not hold in certain cases if the non-adiabatic channel is also included (then one has  $\beta_{tot} = \beta_m - \beta_0 + \beta_{na}$  and  $\beta_{na}$  is positive, see Sec. 5).

All previous considerations have been done near  $T_c$ . At  $T = 0$ , the BCS contribution arising from the  $T_c$  dependency of the superconducting charge-carrier density  $n_s$  (see Eq. (17)) vanishes, because  $\varphi(T = 0) = 1$ . The only contribution to the IE is thus due to magnetic impurities. In the framework of the Abrikosov-Gor'kov theory one can write the isotope coefficient at  $T = 0$  in the form:

$$\beta_m = R_0 \alpha_0 \quad , \quad (25)$$

where  $R_0$  is given in appendix. Note that  $R_0$  is a negative function of  $\Gamma_2$  (the direct scattering amplitude) and  $\Gamma_s = \Gamma_1 - \Gamma_2$  (the spin-flip, or exchange scattering amplitude) as defined by Abrikosov and Gor'kov[49]. The IC of  $\delta$  is thus negative both near  $T_c$  and at  $T = 0$ . This has to be seen in contrast to the IC of  $T_c$  which is always positive (see Fig. 2). Fig. 4 shows the

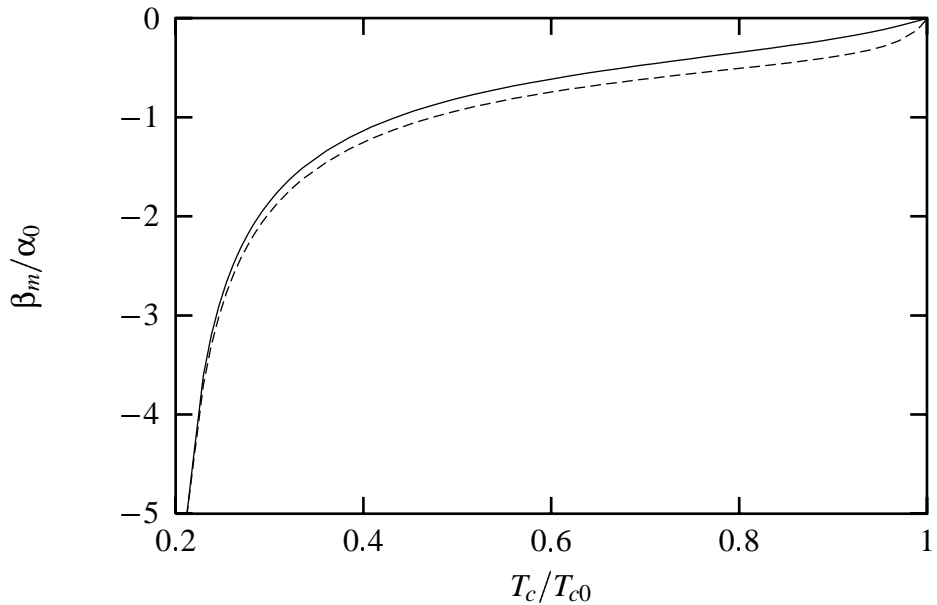


**Figure 4.** Isotope coefficient of the penetration depth at  $T = 0$  in the presence of magnetic impurities (normalized to  $\alpha_0$ ). There is no free parameter in the relation  $\beta_m(T_c)$ . Solid and dashed lines are for  $\Gamma_2/\Gamma_s = 10$  and 50 respectively (see Ref. [6]).

universal relation  $\beta(T_c)$  for two values of  $\Gamma_2$ . One remembers that  $T_c$  is determined by the magnetic impurity concentration.

There are two major differences between the results obtained near  $T_c$  (Fig. 3) and at  $T = 0$  (Fig. 4). First, the direct scattering amplitude  $\Gamma_2$  appears only at  $T = 0$ . Secondly, the IC near  $T_c$  is proportional to  $\alpha_m$  given by Eq. (19), whereas the IC at  $T = 0$  is function of  $\alpha_0$ , the IC of  $T_{c0}$  in the absence of magnetic impurities. This difference is due to the fact that  $\varphi = 1$  at  $T = 0$  (see Eq. (17)) and the penetration depth does consequently not depend on  $T_c$  (the critical temperature in the presence of magnetic impurities).

As shown in Fig. 2, the IC of  $T_c$  fits the data of Zn-doped YBCO. On the other hand, there are no experimental data for conventional superconductors. Furthermore, the magnetic

impurity contribution to the IE of  $\delta$  shown in Fig. 3 has never been measured. It would thus be interesting to perform measurements of these effects, especially since they can be described by universal relations.

## 4 ISOTOPE EFFECT IN A PROXIMITY SYSTEM

In this section we consider another case, a proximity system, in which a factor not related to lattice dynamics induces a change of the isotope coefficient of  $T_c$  and  $\delta$ . Consider an  $S - N$  sandwich where  $S$  ( $N$ ) is a superconducting (normal) film. The value of the critical temperature  $T_c$  and the penetration depth  $\delta$  differ substantially from the values  $T_{c0}$  and  $\delta_0$  of the isolated superconductor  $S$ [58, 59]. We show in the following that the proximity effect also influences the isotope coefficient of  $T_c$  and  $\delta$ .

### 4.1 The Critical Temperature

Let us consider a proximity system composed of a weak-coupling superconductor  $S$  of thickness  $L_S$  and a metal or a semiconductor  $N$  of thickness  $L_N$  (e.g. Nb-Ag). In the framework of the McMillan tunneling model[17], which can be used when  $\delta < L_N \ll \xi_N$  ( $\xi_N = h v_{F;N} / 2\pi T$  is the coherence length of the  $N$ -film as defined in Ref. [60]), the critical temperature  $T_c$  of the  $S - N$  system is related to the critical temperature  $T_{c0}$  of  $S$  by the relation[58]:

$$T_c = T_{c0} \left( \frac{\pi T_{c0}}{2\gamma u} \right)^\rho, \quad \rho = \frac{v_N L_N}{v_S L_S}, \quad (26)$$

where  $\gamma \simeq 0.577$  is Euler's constant. The value of  $u$  is determined by the interplay of the McMillan tunneling parameter  $\Gamma = \Gamma_{SN} + \Gamma_{NS}$  and the average phonon frequency  $\Omega$ . For an almost ideal  $S - N$  contact ( $\Gamma \gg \Omega$ ) one has  $u \simeq \Omega$ . In the opposite limit, when  $\Gamma \ll \Omega$  one obtains  $u \simeq \Gamma$  (see Ref. [58]).

Let us first consider the case  $\Gamma \gg \Omega$ . In the BCS model, one has  $T_{c0} \propto \Omega$ . Thus, according to Eq. (26)  $T_c$  and  $T_{c0}$  have the same dependency on the ionic mass in this limit (because  $T_{c0}/u$  is then independent of  $\Omega$ ). This results in the simple relation  $\alpha_{prox} = \alpha_0$  for the IC of  $T_c$  ( $\alpha_0$  is the isotope coefficient of  $T_c$  for the isolated  $S$ -film).

The opposite situation where  $\Gamma \ll \Omega$  is more interesting since  $u = \Gamma$  is independent of ionic masses. Using Eqs. (1) and (26) one obtains for the isotope coefficient of  $T_c$  in the limit  $\Gamma \ll \Omega$ :

$$\alpha_{prox} = \alpha_0 \left( 1 + \frac{v_N L_N}{v_S L_S} \right). \quad (27)$$

One notes first that whereas the presence of a normal film on the superconductor decreases  $T_c$ , the film induces an *increase* of the isotope coefficient of  $T_c$ . The same is true for the presence of magnetic impurities and for the non-adiabatic IE when  $\partial T_c / \partial n > 0$  (see next section). The second interesting feature of Eq. (27) is that one can modify the value of  $\alpha_{prox}$  by changing the thicknesses of the films. For example, if  $v_N/v_S = 0.8$  and  $L_N/L_S = 0.5$  then  $\alpha_{prox} = 0.28$ . By increasing the thickness of the normal film such that  $L_N = L_S$ , one obtains  $\alpha_{prox} = 0.36$ .

We stress the fact that, as in the previous section on magnetic impurities, the change of the IC is due to a factor not related to lattice dynamics. Therefore, there is no reason for  $\alpha_{prox}$  to be limited to values below 0.5.

To the best of our knowledge the change in the IC caused by the proximity effect has never been measured, even in conventional superconductors. It would be interesting to carry out such experiments in order to observe this phenomenon.

## 4.2 The Penetration Depth

The proximity effect also affects the shielding of a magnetic field. The most dramatic effect of the normal layer on the penetration depth is seen in the low-temperature regime ( $T/T_c \leq 0.3$ ). Although the penetration depth of a pure conventional superconductor is only weakly temperature dependent in this regime ( $\delta^{-2} \sim \varphi = 1 - T^4/T_c^4$ ) the presence of the normal layer induces a temperature dependence through the proximity effect. For the same  $S-N$  proximity system as considered above the penetration depth is given by[59]

$$\delta^{-3} = a_N \Phi \quad , \quad (28)$$

where  $a_N$  is a constant depending only on the material properties of the normal film (it is ionic-mass independent) and

$$\Phi = \pi T \sum_{n \geq 0} \frac{1}{x_n^2 p_n^2 + 1}, \quad p_n = 1 + \varepsilon t \sqrt{x_n^2 + 1} \quad . \quad (29)$$

$x_n = \omega_n/\varepsilon_S(T)$  with  $\omega_n = (2n+1)\pi T$  (the Mastubara frequencies) and  $\varepsilon_S(T)$  is the superconducting energy gap of  $S$ . In the weak-coupling limit considered here,  $\varepsilon_S(0) = \varepsilon\pi T_{c0}$  with  $\varepsilon \simeq 0.56$ . The dimensionless parameter  $t = \ell/S_0$  with  $\ell = L_N/L_0$  and  $S_0 = \Gamma/\pi T_{c0}$  ( $\Gamma \sim 1/L_0$  is the McMillan parameter[17]).  $L_N$  and  $L_0$  are the thickness of the normal film and some arbitrary thickness, respectively (in the following we take  $L_0 = L_S$ , the thickness of the superconducting film). From Eqs. (3) and (28) one obtains the IC of the penetration depth for the proximity system:

$$\beta_{prox} = -\frac{2\alpha_0}{3\Phi} \sum_{n > 0} \frac{x_n^2 p_n^2}{x_n^2 p_n^2 + 1} \left( 1 - \frac{\varepsilon t}{p_n \sqrt{x_n^2 + 1}} \right) \quad , \quad (30)$$

where  $\alpha_0$  is again the IC of  $T_{c0}$  for the superconducting film  $S$  alone. This result has three interesting features. First, as for the case of magnetic impurities, the IC of  $T_c$  and  $\delta$  have opposite signs. This observation is valid as long as one does not mix the different channels presented in this work (magnetic impurities, proximity effect and non-adiabaticity). The addition of a non-adiabatic contribution (next section) may lead to a different conclusion. Secondly, one can see from Eq. (30) that  $\beta_{prox}$  depends on the proximity parameter  $t$ . One can thus modify the IC either by changing the ratio  $\ell = L_N/L_S$  or the McMillan tunneling parameter  $\Gamma$  (e.g. by changing the quality of the interface; see Ref. [6]). Fig. 5 shows this dependence for different temperatures. One notes that, contrary to the value of  $\alpha_{prox}$ , the IC of the penetration depth decreases with increasing ratio  $\ell$ . Finally, one notes that the IC  $\beta_{prox}$  is temperature-dependent. This unconventional feature was also observed for the IC of  $\delta$  in the presence of magnetic impurities near  $T_c$ . Fig. 6 shows the temperature dependence for different values of the parameters. The trend is similar to the case of magnetic impurities:  $|\beta_{prox}|$  increases with increasing  $T$ . Note, however, that the two effects are calculated in very different temperature ranges (near  $T_c$  and near  $T = 0$ ). A complete description of this effect can be found in Ref. [5].

## 5 NON-ADIABATIC ISOTOPE EFFECT

The non-adiabatic isotope effect introduced in Ref. [3] was used in Refs. [3, 4, 5, 6, 7] to describe the unusual behavior of the isotope coefficient in several high-temperature superconductors. The theory also allowed us to describe the large isotopic shift of the ferromagnetic phase transition in manganites [7]. The concept of the non-adiabatic IE relies on the fact that

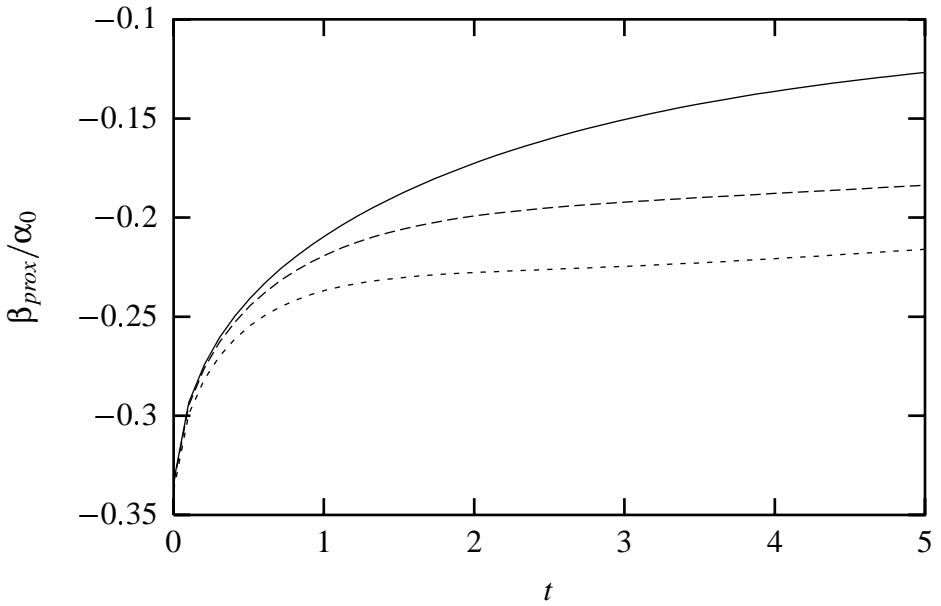


**Figure 5.** Isotope coefficient (normalized to  $\alpha_0$ ) of the penetration depth for a proximity system as a function of  $t$ , for  $T/T_c = 0.1$  (solid), 0.2 (dashed), 0.3 (dotted). See Ref. [6].

in the above-mentioned systems charge-transfer processes involve a non-adiabatic channel. In other words, the electronic ground state of the group of atoms over which the charge-transfer takes place is degenerate, leading to a dynamic Jahn-Teller (JT) effect ( $E_{JT} \leq \hbar\omega$ , where  $E_{JT}$  is the JT energy; see, e.g., Ref. [61]).

The concept of the non-adiabatic isotope effect can be understood by considering two examples: the apex oxygen in high- $T_c$  oxides and the motion of charge-carriers in manganites. Let us first consider high- $T_c$  materials. This system can be seen as a stack of charge reservoirs ( $\text{CuO}$  chains) and conducting subsystems ( $\text{CuO}_2$  planes). Charges are transferred from the reservoir to the conducting layers through the apex oxygen that bridges the two subsystems. Several experiments have shown[62, 63, 64] that the apex oxygen displays a non-adiabatic behaviour. The ion oscillates between two close positions that correspond to two configurational minima of the potential energy surface. These two minima are due to the Jahn-Teller effect since we are dealing with the crossing of electronic terms (see Fig. 7).

The Jahn-Teller effect leads to a “double-well” type potential (which should not be confused with the double-well appearing when the crystal is anharmonic; here we consider energy terms crossing and for each term we use the harmonic approximation). This structure has a strong impact on charge-transfer processes in these materials. Indeed, the motion of charges from the chains to the planes occurs through the apex oxygen. Thus, the charge-transfer process involves the motion of the non-adiabatic ion. The immediate consequence of this observation is that the density of charge-carriers  $n$  in the  $\text{CuO}_2$ -planes (the conducting subsystem) depends on the mass of the non-adiabatic ions involved  $n = n(M)$  (see below).

The situation encountered in manganites is different from the example just described. In these materials, there is no transfer between a reservoir and a conducting subsystem. Instead, the motion of charge-carriers occurs on the Mn-O-Mn complex that displays a non-adiabatic behaviour[65]. As a consequence, the electron hopping involves the motion of the ions and depends on their mass. It was shown in Ref. [7] that this fact can account for the unexpectedly low ferromagnetic critical temperature  $T_{c,f}$ [66] (which is determined by the hopping of the electrons between Mn ions) as well as for the huge isotopic shift of  $T_{c,f}$ [67].

Note that although the charge-transfer processes are different in high-temperature superconductors and in manganites, the formalism described below and in Ref. [68] applies equally well to the two systems. In the following we refer to the example of the apex oxygen. The

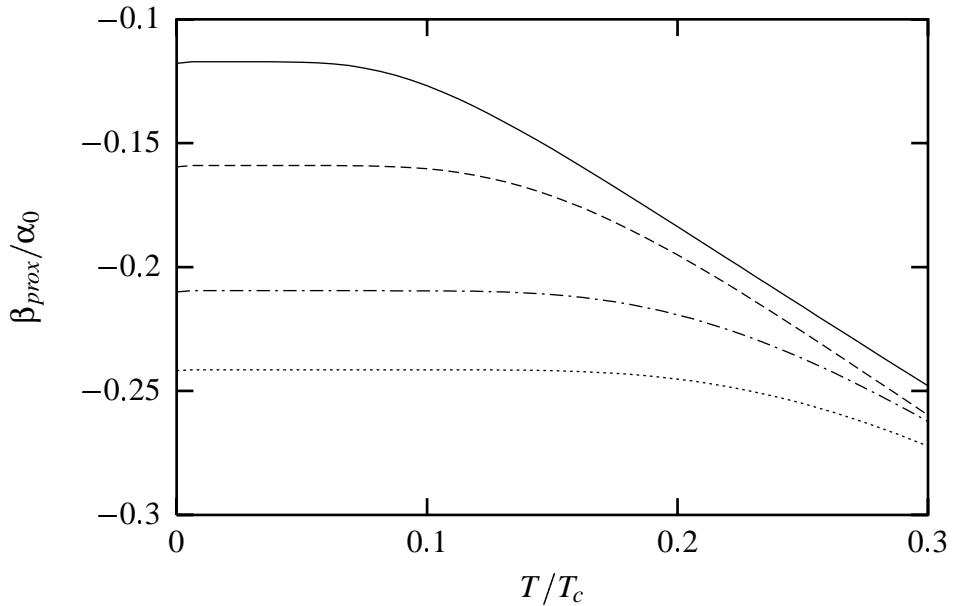


**Figure 6.** Isotope coeff.  $\beta_{prox}$  (normalized to  $\alpha_0$ ) for a proximity system as a function of  $T/T_c$  for  $S_0 = 0.2$ :  $l = 1$  (solid)  $l = 0.5$  (dashed) and  $S_0 = 1$ :  $l = 1$  (dash-dotted)  $l = 0.5$  (dotted). See Ref. [5].

case of manganites can be mapped by replacing “reservoir” and “conducting subsystem” by “Mn ions”.

It is important to realize that the dependence  $n(M)$  is specific to systems where the motion of charges occurs through non-adiabatic ions. In metals, the charge-carriers are not affected by the motion of the ions because of the validity of the adiabatic approximation. We also stress the fact that the apex oxygen is given as a simple example but, as will be shown below, the theory is not limited to this case. Finally, one should note that a phenomenological theory of the IC based on the assumption that  $n = n(M)$  has been proposed in Ref. [69].

To demonstrate that in the presence of non-adiabatic charge-transfer one has  $n = n(M)$ , one best uses the so-called diabatic representation[70] (see also Ref. [68]). Here we only recall the main steps of the calculation. Let us assume that, because of the degeneracy of electronic states (or Jahn-Teller crossing), the potential energy surface  $E(R)$  ( $R$  is the relevant configurational coordinate) of the group of non-adiabatic ions (such as the apex O, in-plane Cu and O for high- $T_c$  materials or Mn and O ions in manganites) has two close minima (see Fig. 7). In the diabatic representation the total wave-function  $\Psi(\mathbf{r}, \mathbf{R}, t)$  ( $\mathbf{r}$  is the electronic coordinate) is written as a linear combination of the wave-functions in the two crossing potential surfaces. The total wave-function cannot be decomposed as a product of electronic and lattice wave-functions. On the other hand, one can write the total wave-function as a sum of symmetric and antisymmetric terms. The energy splitting between these symmetric and antisymmetric terms, which corresponds to the inverse lifetime of oscillations between the configurations (minima of the potential energy surface), has the form[3, 5, 7, 68]:

$$H_{12} = \langle \Psi_1 | H_e | \Psi_2 \rangle \simeq L_0 F_{12} , \quad (31)$$

where  $H_e$  is the electronic part of the total Hamiltonian and

$$L_0 = L(\mathbf{R}_0) = \int d\mathbf{r} \psi_1^*(\mathbf{r}, \mathbf{R}) H_e \psi_2(\mathbf{r}, \mathbf{R}) , \quad (32)$$

$$F_{12} = \int d\mathbf{R} \Phi_1^*(\mathbf{R}) \Phi_2(\mathbf{R}) . \quad (33)$$

The last equality in Eq. (31) is obtained under the assumption that the electronic wave-function  $\psi_i$  ( $i = 1, 2$ ) is a slowly varying functions of  $\mathbf{R}$ .  $L_0$  can then be evaluated at  $\mathbf{R}_0$ ,

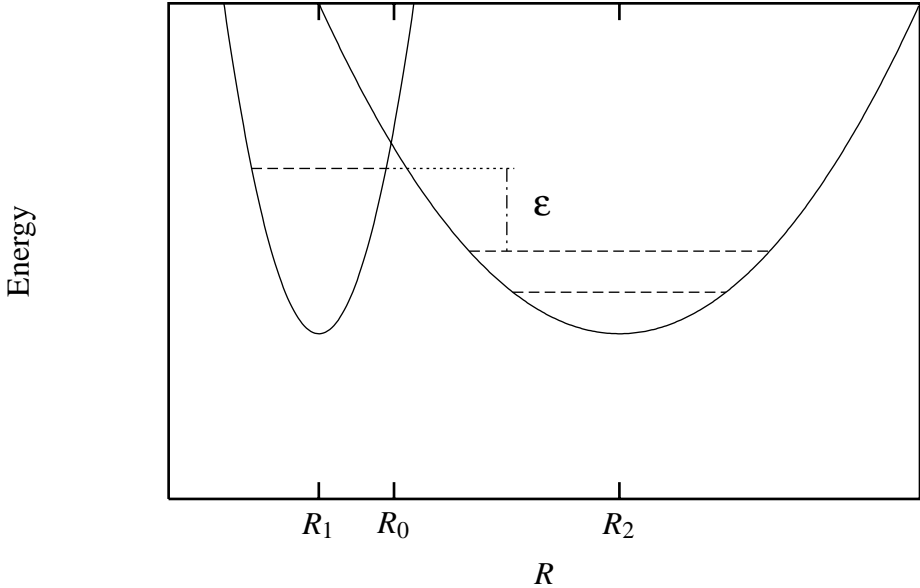


**Figure 7.** Potential energy surface (PES) as a function of the configurational coordinate  $R$ . The crossing of electronic terms leads to a dynamical Jahn-Teller distortion (two minima of the PES).

the crossing of electronic terms, and taken out of the integral over  $\mathbf{R}$ . It does not depend on ionic masses. On the other hand, the important Franck-Condon factor (33) depends on the lattice wave-functions  $\Phi_i(\mathbf{R})$ , and thus on ionic masses. Given the perturbation, Eq. (31), one can calculate the probability of finding the charge-carrier in the conducting layer [3, 5, 7, 68]. Note that non adiabaticity affects the bandwidth of the reservoir and conducting bands rather than the chemical potential (which is the same because of thermodynamic equilibrium). Thus, in the case of YBCO, the plane and chain bands have the same chemical potential, but different widths. This affects the charge-carrier concentration in the two subsystems.

Qualitatively, the charge transfer can be visualized as a multi-step process. First, the charge carrier can move from the reservoir to the group of ions (e.g. from the chains to the apical oxygen in YBCO). Then, the non-adiabatic ions tunnel to the other electronic term ( $\Psi_1 \rightarrow \Psi_2$ ). As a final step, the charge carrier can hop to the conducting layer (from the apical oxygen to the CuO<sub>2</sub> planes). The crucial point of the theory is that as a result of this multi-step process, the probability  $P$  of finding the charge-carrier in the conducting subsystem depends on Eq. (31) and thus on the Franck-Condon factor  $F_{12} = F_{12}(M)$ , Eq. (33), that depends on ionic masses. In other words the charge-carrier concentration  $n$ , which is proportional to the probability  $P$ , depends on the ionic mass  $M$ . It is this unusual dependence  $n = n(M)$ , found in high-temperature superconductors and manganites, that is responsible for the unconventional isotope effect of  $T_c$  and  $\delta$ .

## 5.1 The Critical Temperature

Given that  $n = n(M)$ , we can write the isotope coefficient of  $T_c$  as  $\alpha = \alpha_{ph} + \alpha_{na}$ , where  $\alpha_{ph} = (M/T_c)(\partial T_c/\partial \Omega)(\partial \Omega/\partial M)$  is the usual (BCS) phonon contribution ( $\Omega$  is a characteristic phonon energy) and the non-adiabatic contribution is given by:

$$\alpha_{na} = \gamma \frac{n}{T_c} \frac{\partial T_c}{\partial n} , \quad (34)$$

where the parameter  $\gamma = -M/n(\partial n/\partial M)$  has a weak logarithmic dependence on  $M$  (see Ref. [3]). This parameter should not be confused with Euler's constant. Eq. (34) shows that the IC of  $T_c$  depends on the doping of the conducting layer and on the relation  $T_c(n)$ .

This result was used in Refs. [3, 4] to analyse the IE of high-temperature superconductors (see below).

## 5.2 The Penetration Depth

The concept of the non-adiabatic isotope effect relies on the fact that the charge-carrier concentration depends on the ionic mass because of the Jahn-Teller crossing of electronic terms. Obviously, any quantity that depends on  $n(M)$  will also display an unconventional isotope effect. One such quantity is the penetration depth of a magnetic field  $\delta$  given in Eq. (17). Note that the relation  $\delta^{-2} \sim n_s$  is also valid in the strong-coupling case (see, e.g., Refs. [5]). From Eq. (3) one has

$$\beta \equiv -\frac{M}{\delta} \frac{\partial \delta}{\partial n_s} \frac{\partial n_s}{\partial M} = \frac{M}{2n_s} \frac{\partial n_s}{\partial M} . \quad (35)$$

As mentioned in Sec. 2.7, because of the relation  $n_s = n\varphi(T)$ , one has to distinguish two contributions to  $\beta$ . There is a usual (BCS) phonon contribution,  $\beta_{ph}$ , arising from the fact that  $\varphi(T/T_c)$  depends on ionic mass through the dependency of  $T_c$  on the characteristic phonon frequency. This BCS contribution was discussed in Sec. 2. In the present paper we focus on the non-trivial manifestation of isotopic substitution arising from the isotope dependence of the charge-carrier concentration  $n$ . Such an effect can even be observed in the low-temperature region where  $\varphi \simeq 1$ . From Eq. (35) and the relation  $n_s = n\varphi(T)$  it follows that

$$\beta = \beta_{ph} + \beta_{na} = \frac{M}{2\varphi(T)} \frac{\partial \varphi(T)}{\partial M} + \frac{M}{2n} \frac{\partial n}{\partial M} , \quad (36)$$

where  $n(M)$  is the normal-state charge-carrier concentration. Comparing Eq. (34) and the second term of the right hand side of Eq. (36) one infers that  $\beta_{na} = -\gamma/2$  and thus establish a relation between the non-adiabatic isotope coefficients of  $T_c$  and  $\delta$ :

$$\alpha_{na} = -2\beta_{na} \frac{n}{T_c} \frac{\partial T_c}{\partial n} . \quad (37)$$

This result holds for London superconductors. The equation contains only measurable quantities and can thus be verified experimentally. It is interesting to note that  $\beta_{na}$  and  $\alpha_{na}$  have opposite signs when  $\partial T_c / \partial n > 0$  (which corresponds to the underdoped region of high- $T_c$  materials).

Note, finally, that in the presence of magnetic impurities the relation  $n_s = n\varphi(T)$  remains valid, but  $\varphi(T)$  depends now on the direct scattering amplitude  $\Gamma_2$  defined in Sec. 3.3 (this results, e.g., in the inequality  $n_s(T=0) < n$  in the gapless regime). As a consequence, magnetic impurities affect the first term in Eq. (36) (that now depends on  $\Gamma_2$ ), but leaves  $\beta_{na}$  and thus Eq. (37) unchanged.

## 6 OXYGEN ISOTOPE EFFECT IN HIGH- $T_c$ MATERIALS

In this section we briefly discuss experiments done on high-temperature superconductors in the light of the theory exposed in sections 3 and 5. A detailed study of the oxygen isotope effect in high- $T_c$  materials can be found in Refs. [3, 4, 5, 6].

The oxygen isotope effect of  $T_c$  has been observed in a number of experiments[71, 57, 56, 72, 73]. Here we discuss the results obtained on Pr-doped and oxygen-depleted

$\text{YBa}_2\text{Cu}_3\text{O}_{7-\delta}$  (YPrBCO and YBCO respectively). We also discuss shortly the isotope effect of the penetration depth observed in  $\text{La}_{2-x}\text{Sr}_x\text{CuO}_4$  (LSCO). The analysis of the isotope effect in Zn-doped YBCO has already been presented in Sec. 3.

## 6.1 The Critical Temperature

Let us first consider the isotope coefficient of  $T_c$  for Pr-doped YBCO (YPrBCO). Several experiments have established that the Pr replaces Y which is located between the two  $\text{CuO}_2$  planes of a unit cell. The doping affects YBCO mainly in two ways. First, it was shown that because of the mixed-valence state of Pr, holes are depleted from the  $\text{CuO}_2$  planes (see, e.g., Ref. [74]). Secondly, as for Zn substitution, prae-sodium changes the magnetic impurity concentration of the system[56, 74]. Regarding the IE, these experimental facts imply that through the first effect, the non-adiabatic channel is activated, whereas the second effect leads us to consider the magnetic impurity channel for the calculation of  $\alpha$ . The IE is therefore described by  $\alpha_t = \alpha_{ph} + \alpha_{m+na}$ , where  $\alpha_{ph} = 0.025$ [57] is the phonon contribution, and  $\alpha_{m+na}$  is defined by Eq. (19) with  $\alpha_0$  given by Eq. (34). The resulting expression depends on two parameters  $\gamma$  and  $\tilde{\Gamma}_s$ , characterizing the non-adiabatic and magnetic impurity channels, respectively. The latter quantity has been extracted from a fit to the relation  $T_c(x)$  ( $x$  describes the Pr doping)[74] and is  $\tilde{\Gamma}_s = 123\text{K}$ . The parameter  $\gamma = 0.16$  is determined from the mean-square fit to the experimental data. The result is shown in Fig. 8. The theory is

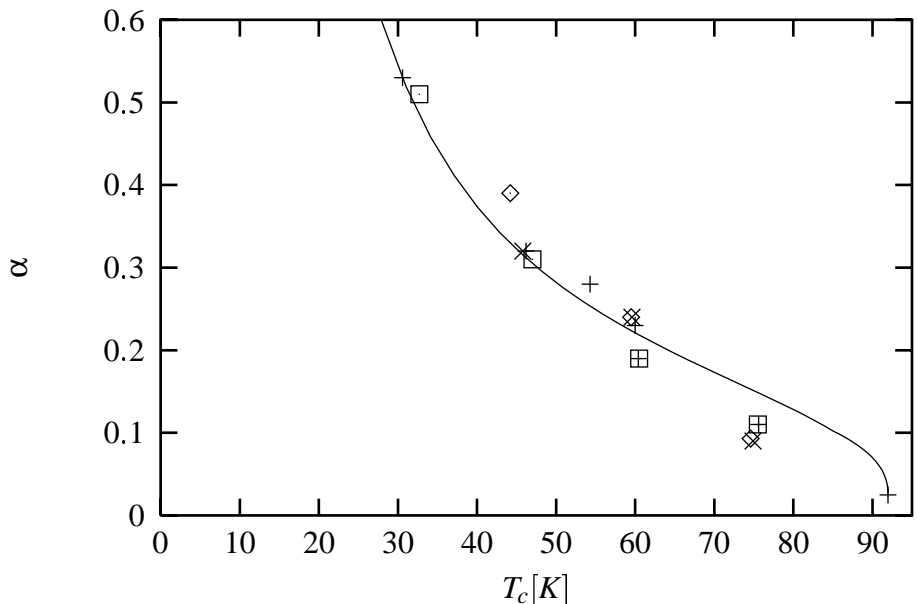


**Figure 8.** Dependence of the isotope coefficient  $\alpha$  on  $T_c$  for  $\text{Y}_{1-x}\text{Pr}_x\text{Ba}_2\text{Cu}_3\text{O}_{7-\delta}$ . Theory: solid line with  $\gamma = 0.16$ ,  $\tilde{\Gamma}_s = 123\text{K}$ ,  $\alpha_0 = 0.025$ ; Experiment: dc magnetization, resistivity and ac susceptibility from Refs. [71, 56].

in good agreement with the experimental data. Note that the negative curvature at high  $T_c$ 's reflects the influence of the non-adiabatic channel (magnetic impurities give a contribution with opposite curvature), whereas the positive curvature seen at low  $T_c$  is due to the presence of magnetic impurities[5].

Oxygen-depleted YBCO is very similar to the previous case in that oxygen depletion both introduces magnetic impurities into the system and removes holes from the  $\text{CuO}_2$  planes. The same equations as above can thus be used, however, with appropriate values of the parameters. The result is shown in Fig. 9, together with the experimental data from Ref. [57]. Note the sharp drop observed near  $T_c = 60\text{K}$ . This drop and the peak above it are related to the presence of a plateau in the dependence  $T_c(n)$  near  $T_c = 60\text{K}$  (see, e.g., Ref. [57]). Since

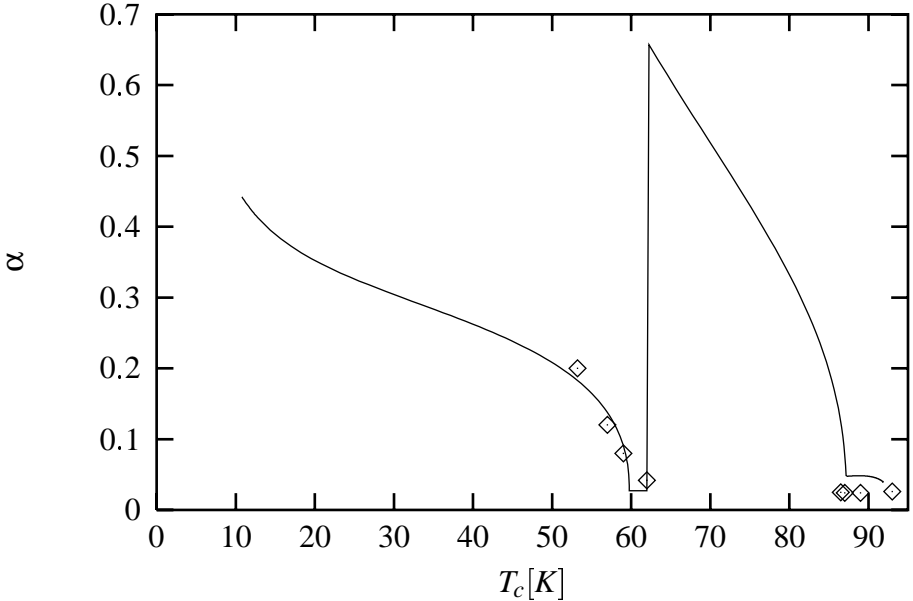


**Figure 9.** Dependence of the isotope coefficient  $\alpha$  on  $T_c$  for  $\text{YBa}_2\text{Cu}_3\text{O}_{6+x}$ . Theory: solid line with  $\gamma = 0.28$ ,  $\tilde{\Gamma}_s = 15\text{K}$ ,  $\alpha_0 = 0.025$ ; Experiment: points from Ref. [57].

Eq. (34) contains the derivative  $\partial T_c / \partial n$ ,  $\alpha_{na}$  will be nearly zero at  $60\text{K}$ . As one increases  $T_c$ , the slope of  $T_c(n)$  jumps to a large value, and decreases again to zero as  $T_c \rightarrow 90\text{K}$ . This behavior of  $T_c(n)$  explains the maximum appearing in  $\alpha_{na}(T_c)$  above  $60\text{K}$ . The peak structure is thus specific to oxygen-depleted YBCO because neither YPrBCO nor YBCZnO display such a plateau in the relation  $T_c(n)$ . It would be interesting to verify this result, by measuring the oxygen isotope effect between  $60$  and  $90\text{K}$ .

The main difference between Pr-substituted (Fig. 8) and oxygen-depleted YBCO (Fig. 9) lies in the fact that the doping affects different ions of the system. Magnetic impurities are introduced at different sites (on Y for the first material and in the chains or the apical oxygen position for the second system). Furthermore, non-adiabatic charge-transfer processes involve mainly Pr as well as Cu and O of the planes in YPrBCO, whereas they involve mainly the apical O in oxygen-depleted YBCO (to a lower extent, chain and in plane O and Cu are also involved).

Contrary to YPrBCO, it is not possible to extract the value of  $\tilde{\Gamma}_s$  (the contribution of magnetic impurities). The best fit to the few data gives  $\gamma = 0.28$  and  $\tilde{\Gamma}_s = 15\text{K}$ . Two important points have to be noted concerning these values. First, because of the limited data available, the values may vary, although the order of magnitude will remain (see also Ref.[6]). The other remark concerns the value of  $\tilde{\Gamma}_s$  for YPrBCO and YBCO. From these values one concludes that oxygen depletion introduces a smaller amount of magnetic moments than Pr doping. It would be interesting to perform more isotope effect experiments on oxygen-depleted YBCO and to determine the effective magnetic moment per depleted oxygen through other means.

## 6.2 The Penetration Depth

The only experimental observation of the isotopic shift of the penetration depth has been done on  $\text{La}_{2-x}\text{Sr}_x\text{CuO}_4$  (LSCO)[73]. There are no data available on YBCO-related materials. Since only Pr-doped YBCO has one free parameter ( $\gamma$ ) we present the results of our theoretical calculations only in this case. The oxygen-depleted case was studied as a function of the two parameters  $\gamma$  and  $\tilde{\Gamma}_s$  in Ref. [5].

Let us begin with the case of LSCO. This case is simpler to study than YBCO related materials, since no significant amount of magnetic impurities has been detected in this ma-

terial. Our analysis can thus be carried out with Eqs. (34) or (37). The isotope coefficient has been measured for Sr concentrations near  $x \approx 0.11$  and  $x \approx 0.15$ . The first concentration corresponds to the region where  $T_c(x)$  experiences a small dip. The origin of this dip is not well-established but is probably related to electronic inhomogeneities and structural instability. Since many factors affect  $T_c$  at this Sr concentration, it is difficult to interpret correctly the isotope effect of  $T_c$  and  $\delta$ .

The second concentration at which an isotope shift of  $\delta$  has been measured is at optimal doping ( $T_c$  is maximal). The experimental shift  $\Delta\delta/\delta \simeq 2\%$  and Eq. (3) allows one to determine the value of  $\beta_{na} \simeq 0.16$  and thus  $\gamma \simeq 0.32$  through Eq. (37). This result is in good agreement with the values obtained for Pr-doped and O-depleted YBCO (see Ref. [6] for a discussion on LSCO).

Let us now turn to the isotope coefficient of the penetration depth for YBCO-related materials. From the evaluation of the parameter  $\gamma$  (see Eq. (34) and above) and from Eq. (37) one obtains the non-adiabatic contribution to the IC of the penetration depth in Pr-doped and O-depleted YBCO. One obtains  $\beta_{na} = -0.08$  in the first case and  $\beta_{na} = -0.14$  in the second.

Using Eqs. (19), (22) and (34), as well as the values of the parameters  $\gamma$  and  $\tilde{\Gamma}_s$  given above, one can calculate the IC resulting from the contributions of magnetic impurities and non-adiabaticity for YPrBCO near  $T_c$ . The result is shown in Fig. 10 for three different temperatures. One notes that contrary to the case of magnetic impurities alone (one sets

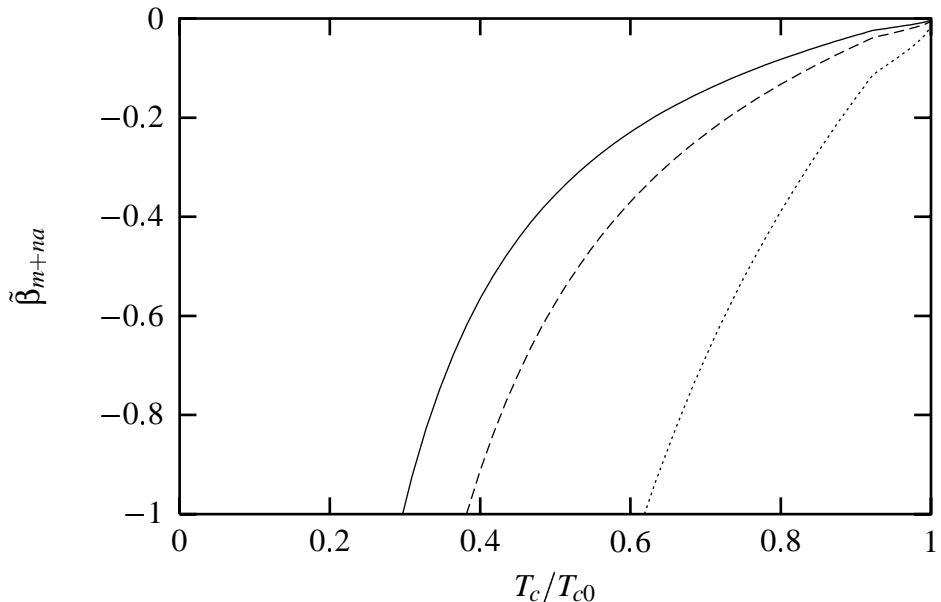


**Figure 10.** Dependence of the isotope coefficient  $\tilde{\beta}_{m+na}$  on  $T_c$  for  $T/T_c = 0.75$  (solid line), 0.85 (dashed), 0.95 (dotted).  $\alpha_0 = 0.025$ ,  $\gamma = 0.16$ , and  $\tilde{\Gamma}_s = 123\text{K}$  (parameters for  $\text{Y}_{1-x}\text{Pr}_x\text{Ba}_2\text{Cu}_3\text{O}_{7-\delta}$ ).

$\gamma = 0$ ) studied in Sec. 3 (Figs. 2 and 3), the isotope effect of the penetration depth does not have the same qualitative behaviour as the IC of  $T_c$  (compare Figs. 9 and 10). The change of curvature does not take place at the same value of  $T_c$  (in the case of  $\tilde{\beta}_{m+na}$  the change occurs at high  $T_c$ 's and is barely visible on the figure; see Ref. [6] for a discussion of this point). One should measure the IC of  $\delta$  for YPrBCO and YBCO, since it would allow one to give a better estimate of the parameters and to test the theory.

## 7 CONCLUSIONS

We have reviewed different aspects of the isotope effect. In a first part, we have summarized the main theories developed to explain the isotope effect in conventional superconductors

and we have discussed their relevance for high- $T_c$  oxides. In particular, we have considered the effect of the Coulomb interaction, band structure (van Hove singularities), multiaatomic compounds, anharmonicity and non-phononic mechanisms on the value of the isotope coefficient. These effects can account for most experimental data obtained on conventional superconductors. For example, they allow one to describe the deviation from the standard BCS value  $\alpha = 0.5$  in transition metals or the inverse isotope effect ( $\alpha < 0$ ) found in PdH. The results show clearly that a vanishing or even a negative isotope coefficient can be obtained within conventional superconductivity where the pairing between charge-carriers is mediated by the electron-phonon interaction. Generally, however, the small isotope coefficient is obtained only in conjunction with low  $T_c$ 's. On the other hand, one can also obtain values of the isotope coefficient that are larger than  $\alpha = 0.5$  when anharmonic or band-structure effects are present in the system.

In a second part, we have analyzed the effect of magnetic impurities, proximity contacts and non-adiabatic charge-transfer processes on the isotope coefficient (see also Refs. [3, 4, 5, 6, 7]). An important common feature of these factors is that they are not related to the pairing mechanism but, nevertheless, strongly affect the isotope effect. One notes that  $\alpha > 0.5$  is allowed in all three channels. Furthermore, these factors can induce a non-trivial isotopic shift of quantities such as the penetration depth  $\delta$ . In the case of magnetic impurities and the proximity effect, the isotope effect of the penetration depth is temperature dependent. This phenomenon has not been investigated experimentally yet. In the presence of non-adiabaticity, we have established a relation between the isotope shift of  $T_c$  and  $\delta$  for London superconductors.

The theory presented in the second part of this review allowed us to describe the unconventional behavior of the isotope coefficient in  $\text{YBa}_2\text{Cu}_3\text{O}_7$  related systems (Zn and Pr-substituted as well as oxygen-depleted materials). The case of Zn-substituted YBCO was described by involving solely the magnetic impurity channel and did not require any fitting parameter. The theoretical curve also applies to conventional superconductors.

Our calculations suggest several experiments both on conventional and high-temperature superconductors. In particular, it would be interesting to measure the change of the isotope coefficient induced by a proximity system or magnetic impurities in conventional superconductors to test our theory. Furthermore, more experiments have to be done on high-temperature superconductors so as to determine more precisely the parameters appearing in the theory.

## 8 Acknowledgment

A.B. is grateful to the Naval Research Laboratory and the Swiss National Science Foundation for the support. The work of V.Z.K. is supported by the U.S. Office of Naval Research under contract No. N00014-96-F0006.

## 9 APPENDIX

We derive the explicit form of the function  $R_0$  given in Eq. (25) (see Ref. [6]). The penetration depth calculated by Skalski *et al.* at zero temperature is given by  $\delta^{-2} = -(4\pi ne^2/mc^2)\tilde{K}(\omega = 0, \mathbf{q} = 0)$  with[50]

$$\tilde{K}(0, 0) = -\frac{1 + \bar{\Gamma}\bar{\eta}^{-3}}{\bar{\eta}} \left[ \frac{\pi}{2} - \frac{f(\bar{\eta})}{R(\bar{\eta})} \right] + \bar{\Gamma}\bar{\eta}^{-3} \left[ \frac{2}{3}\bar{\eta} - \frac{\pi}{4}\bar{\eta} + 1 \right] \quad (38)$$

for  $\bar{\Gamma}, \bar{\eta} < 1$  (with  $f(\bar{\eta}) = \arccos\bar{\eta}$ ) or  $\bar{\Gamma} < 1, \bar{\eta} > 1$  (with  $f(\bar{\eta}) = \text{arcosh}\bar{\eta}$ ) and

$$\begin{aligned}\tilde{K}(0,0) = & -\frac{1+\bar{\Gamma}\bar{\eta}^{-3}}{\bar{\eta}} \left\{ \frac{\pi}{2} - 2\frac{\bar{\Gamma}-1}{R(\bar{\Gamma})} - R^{-1}(\bar{\eta})(\text{arcosh}\bar{\eta} - 2\text{artanh}\mathcal{R}) \right\} \\ & + \bar{\eta}^{-3} \left\{ \left( \frac{2}{3}\bar{\eta}^2 + 1 \right) (\bar{\Gamma} - R(\bar{\Gamma})) - \frac{1}{2}\eta R(\bar{\Gamma}) \left( \frac{2}{3}\eta - 1 \right) - \bar{\eta}\bar{\Gamma} \left( \frac{\pi}{4} - \frac{\bar{\Gamma}-1}{R(\bar{\Gamma})} \right) \right\}\end{aligned}\quad (39)$$

for  $\bar{\Gamma}, \bar{\eta} > 1$ . We have introduced the notation  $\bar{\Gamma} = \Gamma_s/\Delta$ ,  $\bar{\eta} = \eta\bar{\Gamma} = \Gamma_2/\Delta$ ,  $\eta = \Gamma_2/\Gamma_s$ ,  $R(x) = \sqrt{|1-x^2|}$  with  $x = \bar{\Gamma}, \bar{\eta}$  and  $\mathcal{R} = [(\bar{\Gamma}-1)(\bar{\eta}-1)/(\bar{\Gamma}+1)(\bar{\eta}+1)]^{1/2}$ .  $\Delta \equiv \Delta(T=0, \Gamma_s)$  is the order parameter in the presence of magnetic impurities. Eqs. (38),(39) are valid when  $\Gamma_s \ll \Gamma_2$ . These two scattering amplitudes,  $\Gamma_2$  and  $\Gamma_s$  ( $\Gamma_s = \Gamma_1 - \Gamma_2$ ), defined by Abrikosov and Gor'kov[49], describe the direct and exchange scattering, respectively. One can calculate the magnetic impurity contribution to the IC at  $T=0$  from Eq. (3) in a straightforward way using Eqs. (38) and (39). The result can be written as

$$\beta_m(T=0) = -\frac{\alpha_\Delta}{2} \frac{K_1 + K_2}{\tilde{K}(0,0)} \quad (40)$$

where  $\alpha_\Delta$  is defined below,  $\tilde{K}(0,0)$  is given by Eqs. (38), (39) and

$$\begin{aligned}K_1 &= -\frac{1+3\bar{\Gamma}\bar{\eta}^{-3}}{\bar{\eta}} \left( \frac{\pi}{2} - \frac{f(\bar{\eta})}{R(\bar{\eta})} \right) \pm \frac{1+\bar{\Gamma}\bar{\eta}^{-3}}{R(\bar{\eta})^2} \left( \frac{\bar{\eta}}{R(\bar{\eta})} f(\bar{\eta}) - 1 \right) \\ K_2 &= \bar{\Gamma}\bar{\eta}^{-3} \left( 2 - \frac{\pi}{4}\bar{\eta} \right)\end{aligned}\quad (41)$$

for  $\bar{\Gamma}, \bar{\eta} < 1$  (upper sign,  $f(\bar{\eta}) = \arccos\bar{\eta}$ ) or  $\bar{\Gamma} < 1, \bar{\eta} > 1$  (lower sign,  $f(\bar{\eta}) = \text{arcosh}\bar{\eta}$ ) and

$$\begin{aligned}K_1 &= -\frac{1+3\bar{\Gamma}\bar{\eta}^{-3}}{\bar{\eta}} \left\{ \frac{\pi}{2} - 2\frac{\bar{\Gamma}-1}{R(\bar{\Gamma})} - \frac{1}{R(\bar{\eta})} (\text{arcosh}\bar{\eta} - 2\text{artanh}\mathcal{R}) \right\} - \frac{1+\bar{\Gamma}\bar{\eta}^{-3}}{\bar{\eta}} \left\{ 2\frac{\bar{\Gamma}(\bar{\Gamma}-1)}{R(\bar{\Gamma})^3} \right. \\ &\quad \left. - \frac{1}{R(\bar{\eta})} \left[ \frac{\bar{\eta}}{R(\bar{\eta})^2} (\text{arcosh}\bar{\eta} - 2\text{artanh}\mathcal{R}) + \frac{\mathcal{R}}{1-\mathcal{R}^2} \left( \frac{\bar{\Gamma}^2}{R(\bar{\Gamma})^2} + \frac{\bar{\eta}^2}{R(\bar{\eta})^2} \right) - \frac{\bar{\eta}}{R(\bar{\eta})} \right] \right\} \\ K_2 &= \frac{3}{\bar{\eta}^3} \left( \frac{2}{3}\bar{\eta}^2 + 1 \right) [\bar{\Gamma} - R(\bar{\Gamma})] - \frac{1}{2}\eta R(\bar{\Gamma}) \left( \frac{2}{3}\eta^2 - 1 \right) - \bar{\eta}\bar{\Gamma} \left( \frac{\pi}{4} - \frac{\bar{\Gamma}-1}{R(\bar{\Gamma})} \right) \\ &\quad + \frac{1}{\bar{\eta}^3} \left\{ \left[ \frac{\bar{\Gamma}}{R(\bar{\Gamma})} \left( \frac{2}{3}\bar{\eta}^2 + 1 \right) - \frac{4}{3}\bar{\eta}^2 \right] [\bar{\Gamma} - R(\bar{\Gamma})] \right. \\ &\quad \left. + \frac{1}{2}\eta \frac{\bar{\Gamma}^2}{R(\bar{\Gamma})} \left( \frac{2}{3}\eta^2 - 1 \right) + 2\bar{\eta}\bar{\Gamma} \left[ \frac{\pi}{4} - \frac{\bar{\Gamma}-1}{R(\bar{\Gamma})} \left( 1 + \frac{\bar{\Gamma}}{2R(\bar{\Gamma})^2} \right) \right] \right\}\end{aligned}\quad (42)$$

for  $\bar{\Gamma}, \bar{\eta} > 1$  and  $\Delta T_c/T_c(\bar{\Gamma}-1) \ll 1$ . The last condition expresses the fact that the calculation is not valid in the immediate vicinity of  $\bar{\Gamma} = 1$ . Eq. (40) contains  $\alpha_\Delta$  which is the IC of the order parameter  $\Delta$ . In strong-coupling systems,  $\alpha_\Delta$  has to be calculated numerically using Eliashberg's equations. Here we calculate the IC in the framework of the BCS model where  $\alpha_\Delta$  can be calculated analytically. Indeed, from the relations

$$\ln \left( \frac{\Delta}{\Delta_0} \right) = \begin{cases} -\frac{\pi}{4}\bar{\Gamma} & : \bar{\Gamma} \leq 1 \\ -\ln [\bar{\Gamma} + R(\bar{\Gamma})] + \frac{R(\bar{\Gamma})}{2\bar{\Gamma}} - \frac{\bar{\Gamma}}{2} \arctan R(\bar{\Gamma})^{-1} & : \bar{\Gamma} > 1 \end{cases}, \quad (43)$$

derived by Abrikosov and Gor'kov [ $\Delta_0 = \Delta(T=0, \Gamma_s=0)$  is the order parameter in the absence of magnetic impurities] one obtains

$$\alpha_\Delta = \alpha_{\Delta_0} \begin{cases} \left( 1 - \frac{\pi}{4}\bar{\Gamma} \right)^{-1} & : \bar{\Gamma} \leq 1 \\ \left[ 1 - \frac{\bar{\Gamma}}{2} \arctan R(\bar{\Gamma})^{-1} - \frac{R(\bar{\Gamma})}{2\bar{\Gamma}} \right]^{-1} & : \bar{\Gamma} > 1 \end{cases}. \quad (44)$$

In the BCS approximation one further has  $\alpha_{\Delta_0} = \alpha_0$ , where the last quantity was defined before as the IC of  $T_{c0}$ , that is, in the absence of magnetic impurities.

Finally, one obtains Eq. (25) with  $R_0$  given by:

$$R_0 = -\frac{\alpha_{\Delta}}{2\alpha_0} \frac{K_1 + K_2}{\tilde{K}(0,0)} \quad (45)$$

and  $\alpha_{\Delta}$  is given by Eq. (44).

## References

- [1] H. Fröhlich, *Phys. Rev.* **79**, 845 (1950).
- [2] (a) E. Maxwell, *Phys. Rev.* **78**, 477 (1950); C.A. Reynolds, B. Serin, and L.B. Nesbitt, *Phys. Rev.* **84**, 691 (1951); (b) J.L. Olsen, *Cryogenics* **2**, 356 (1963); (c) B.T. Matthias, T.H. Geballe, E. Corenzwit, and G.W. Hull Jr., *Phys. Rev.* **128**, 588 (1962); (d) R.A. Hein, and J.W. Gibson *Phys. Rev.* **131**, 1105 (1963); (e) E. Bucher, J. Müller, J.L. Olsen, and C. Palmy *Phys. Lett.* **15**, 303 (1965)
- [3] V.Z. Kresin, and S.A. Wolf, *Phys. Rev. B* **49**, 3652 (1994); and in *Anharmonic Properties of High- $T_c$  Cuprates*, p. 18, D. Mihailovic, G. Ruani, E. Kaldis, K.A. Müller, Eds., World Scientific (1995).
- [4] V.Z. Kresin, A. Bill, S.A. Wolf, and Yu.N. Ovchinnikov, *Phys. Rev. B* **56**, 107 (1997); *J. Supercond.* **10**, 267 (1997).
- [5] A. Bill, V.Z. Kresin, and S.A. Wolf, *Z. Phys. Chem.* **201**, 271 (1997); *Z. Phys. B*, in press.
- [6] A. Bill, V.Z. Kresin, and S.A. Wolf, *preprint*.
- [7] V.Z. Kresin, and S.A. Wolf, *Phil. Mag. B* **76**, 241 (1997).
- [8] J.P. Franck, *Physica Scripta* **T66**, 220 (1996); J.P. Franck, S. Harker, and J.H. Brewer, *Phys. Rev. Lett.* **71**, 283 (1993); J.P. Franck, and D.D. Lawrie, *Physica C* **235-240**, 1503 (1994); *J. Supercond.* **8**, 591 (1995); *J. Low Temp. Phys.* **105**, 801 (1996).
- [9] G.M. Zhao, V. Kirtikar, K.K. Singh, A.P.B. Sinha, and D.E. Morris, *Phys. Rev. B* **54**, 14956 (1996).
- [10] G. Gladstone, M.A. Jensen, and J.R. Schrieffer, Superconductivity in transition metals, in: *Superconductivity*, R.D. Parks, ed., Marcel Dekker, New York (1967).
- [11] E.A. Lynton. *Superconductivity*, Methuen, London (1969).
- [12] R.D. Fowler, J.D.G. Lindsay, R.W. White, H.H. Hill, and B.T. Matthias, *Phys. Rev. Lett.* **19**, 892 (1967).
- [13] N. Bogolyubov, N. Tolmachev, and D. Shirkov. *A New Method in the Theory of Superconductivity*, Cons. Bureau, New-York (1959).
- [14] I.M. Khalatnikov, and A.A. Abrikosov, *Adv. in Physics* **8**, 45 (1959).
- [15] J.C. Swihart, *Phys. Rev.* **116**, 45 (1959); *IBM J. Res. Develop.* **6**, 14 (1962).
- [16] P. Morel and P.W. Anderson, *Phys. Rev.* **125**, 1263 (1962).

- [17] W.L. McMillan, *Phys. Rev.* **167**, 331 (1968); **174**, 537 (1968).
- [18] V.Z. Kresin, *Phys. Lett. A* **122**, 434 (1987).
- [19] J.W. Garland, *Phys. Rev. Lett.* **11**, 114 (1963).
- [20] R. Meservey, and B.B. Schwartz, in Ref. [10].
- [21] E. Schachinger, M.G. Greeson, and J.P. Carbotte, *Phys. Rev. B* **42**, 406 (1990); J.P. Carbotte, and E.J. Nicol *Physica C* **185-189**, 162 (1991).
- [22] J. Labbé, and J. Bok, *Europhys. Lett.* **3** 1225 (1987).
- [23] A.A. Abrikosov, *Physica C* **233** (1994) 102.
- [24] T. Hocquet, J.-P. Jardin, P. Germain, and J. Labbé, *Phys. Rev. B* **52** (1995) 10330.
- [25] T. Dahm, D. Manske, D. Fay, and T. Tewordt, *Phys. Rev. B* **54**, 12006 (1996).
- [26] V.H. Crespi, and M. L. Cohen, *Phys. Rev. B* **48**, 398 (1993).
- [27] A.A. Maradudin, E.W. Montroll, G.H. Weiss, and I.P. Ipatova. *Theory of Lattice Dynamics in the Harmonic Approximation*, Acad. Press, New York (1971).
- [28] V.Z. Kresin, H. Morawitz, and S.A. Wolf. *Mechanisms of Conventional and High-T<sub>c</sub> Materials*, Oxford Univ. Press, New York (1993).
- [29] D. Rainer, and F.J. Culeutto, *Phys. Rev. B* **19**, 2540 (1979); F.J. Culeutto, and F. Pobell, *Phys. Rev. Lett.* **40**, 1104 (1978).
- [30] P. Auban-Senzier, C. Bourbonnais, D. Jerome, C. Lenoir, and P. Batail, *Synthetic Metals* **55-57**, 2542 (1993); J.C.R. Faulhaber, D.Y.K. Ko, and P.R. Briddon, *Synthetic Metals* **60**, 227 (1993).
- [31] B. Ashauer, W. Lee, D. Rainer, and J. Rammer, *Physica B* **148**, 243 (1987).
- [32] T.W. Barbee III, M.L. Cohen, L.C. Bourne, and A. Zettl, *J Phys. C* **21**, 5977 (1988).
- [33] B. Stritzker, and W. Buckel, *Z. Phys.* **257**, 1 (1972); T. Stoskiewicz, *Phys. Status Solidi A* **11**, K123 (1972).
- [34] B.N. Ganguly, *Z. Phys.* **265**, 433 (1973); *Z. Phys. B* **22**, 127 (1975); B.M. Klein, E. N. Economou, and D.A. Papaconstantopoulos *Phys. Rev. Lett.* **39**, 574 (1977); D.A. Papaconstantopoulos, B.M. Klein, E. N. Economou, and L.L. Boyer *Phys. Rev.* **17**, 141 (1978); R.J. Miller, and C.B. Satterthwaite *Phys. Rev. Lett.* **34**, 144 (1975); B.M. Klein, and R.E. Cohen *Phys. Rev. B* **45**, 12405 (1992); M. Yussouff, B.K. Rao, and P. Jena *Solid State Comm.* **94**, 549 (1995).
- [35] S.L. Drechsler, and N.M. Plakida *Phys. Stat. Sol.* **144**, K113 (1987); T. Galbaatar, S.L. Drechsler, N.M. Plakida, and G.M. Vujičić, *Physica C* **176**, 496 (1991).
- [36] K.A. Müller, *Z. Phys. B* **80**, 193 (1990).
- [37] M. Cyrot *et al.*, *Phys. Rev. Lett.* **72**, 1388 (1994); D.S. Fisher, A.J. Millis, B. Shraiman, and R.N. Bhatt, *Phys. Rev. Lett.* **61**, 482 (1988).
- [38] L. Jansen, *private communication*. We thank Prof. Jansen for drawing our attention to this effect.

- [39] T. Nakajima, T. Fukamachi, O. Terasaki, and S. Hosoya, *J. Low Temp. Phys.* **27**, 245 (1977).
- [40] N.W. Ashcroft, and M. Cyrot, *Europhys. Lett.* **23**, 605 (1993); Yu.N. Garstein, A.A. Zakhidov, and E.M. Conwell, *Phys. Rev. B* **49**, 13299 (1994); A.P. Ramirez *et al.*, *Phys. Rev. Lett.* **68**, 1058 (1992); T.W. Ebbesen *et al.*, *Nature* **355**, 620 (1992); P. Auban-Senzier *et al.*, *Synthetic Metals* **55-57**, 3027 (1993).
- [41] W.A. Little, *Phys. Rev.* **134**, A1416 (1964); V. Ginzburg, *Sov. Phys.-JETP* **20**, 1549 (1965); B. Geilikman, *Sov. Phys.-JETP* **48**, 1194 (1965).
- [42] H.-B. Schlüter, and C.-H. Pao, *Phys. Rev. Lett.* **75**, 4504 (1995); *J. Supercond.* **8**, 633 (1995).
- [43] V.Z. Kresin, and H. Morawitz, *Solid State Comm.* **74**, 1203 (1990).
- [44] V.Z. Kresin, and H. Morawitz, *Phys. Rev. B* **37**, 7854 (1988)
- [45] B.T. Geilikman, V.Z. Kresin, and N.F. Masharov, *J. Low Temp. Phys.* **18**, 241 (1975).
- [46] S.A. Wolf, and V.Z. Kresin, in Ref. [3]b, p. 232.
- [47] S. Banerjee, A.N. Das, and D.K. Ray, *Phys. Lett. A* **214**, 89 (1996); *J. Phys. C* **8**, 11131 (1996); S. Sil, and A.N. Das, *J. Phys. C* **9**, 3889 (1997).
- [48] F. Marsiglio, R. Akis, and J.P. Carbotte, *Solid State Comm.* **64**, 905 (1987)
- [49] A. Abrikosov, and L. Gork'ov, *Sov. Phys. JETP* **12**, 1243 (1961).
- [50] S. Skalski, O. Betbeder-Matibet, and P.R. Weiss, *Phys. Rev.* **136**, 1500 (1963).
- [51] J. Carbotte *et al.* *Phys. Rev. Lett.* **66** (1991) 1789.
- [52] S.P. Singh *et al.*, *J. Supercond.* **9**, 269 (1996); K. Hanzawa, *J. Phys. Soc. Japan* **63**, 2494 (1994); S.P. Singh *et al.*, *J. Supercond.* **9**, 269 (1996).
- [53] S. Zagoulev *et al.* *Phys. Rev. B* **52**, 10474 (1995); *Physica C* **259**, 271 (1996).
- [54] C. Panagopoulos, J.R. Cooper, N. Athanassopoulou, and J. Chrosch, *Phys. Rev. B* **54** (1996) 12721.
- [55] R.B. Schwarz, P.J. Yvon, and D. Coffey, in *Studies of High Temperature Superconductors*, vol. **9**, Narlikar, ed., Nova Science Publ., New York (1992); M.K. Crawford, M.N. Kunchur, W.E. Farneth, M.McCarron III, and S.J. Poon, *Phys. Rev. B* **41**, 282 (1990); B. Batlogg *et al.*, *Phys. Rev. Lett.* **59**, 912 (1987); T.A. Faltens *et al.*, *Phys. Rev. Lett.* **59**, 915 (1987).
- [56] G. Soerensen, and S. Gygax , *Phys. Rev. B* **51**, 11848 (1995).
- [57] D. Zech, K. Conder, H. Keller, E. Kaldis, and K.A. Müller, *Physica B* **219&220**, 136 (1996).
- [58] V. Kresin, *Phys. Rev. B* **25**, 157 (1982).
- [59] V. Kresin, *Phys. Rev. B* **32**, 145 (1985).
- [60] J. Clarke, *Proc. R. Soc. London, Ser. A* **308**, 447 (1969).

- [61] L. Salem. *The Molecular Orbital Theory of Conjugated Systems*, Benjamin, New York (1966).
- [62] R.P. Sharma, T. Venkatesan, Z.H. Zhang, J.R. Liu, *Phys. Rev. Lett.* **77**, 4624 (1997).
- [63] J. Mustre de Leon et al., *Phys. Rev. Lett.* **64**, 2575 (1990); L. Gasparov et al., *J. Supercond.* **8**, 27 (1995); G. Ruani et al., *Solid State Comm.* **96**, 653 (1995); A. Jesowski et al., *Phys. Rev. B* **52**, 7030 (1995).
- [64] D. Haskel, E.A. Stern, D.G. Hinks, A.W. Mitchell, and J.D. Jorgensen, *Phys. Rev. B* **56** (1997) 521.
- [65] R.P. Sharma, G.C. Xiang, C. Ramesh, R.L. Greene, and T. Venkatesan, *Phys. Rev. B* **54**, 10014 (1996).
- [66] G. Jonker, and J. van Santen, *Physica* **16**, 337 (1950).
- [67] G.M. Zhao, K. Conder, H. Keller, and K.A. Müller, *Nature* **381**, 676 (1996).
- [68] V.Z. Kresin, *this volume*.
- [69] T. Schneider, and H. Keller, *Phys. Rev. Lett.* **69**, 3374 (1993); *Int. Journ. Mod. Phys. B* **8**, 487 (1993).
- [70] T.F. O'Malley, *Phys. Rev.* **162** (1967) 98; *Adv. Atomic Molec. Phys.* **7**, 223 (1971).
- [71] J.P. Franck, J. Jung, M.A-K. Mohamed, S. Gygax, and G.I. Sproule, *Phys. Rev. B* **44**, 5318 (1991); in *High- $T_c$  Superconductivity, Physical Properties, Microscopic Theory and Mechanisms*, J. Ashkenazi et al. eds. (Plenum Press, New-York, 1991), p. 411.
- [72] H.J. Bornemann and D.E. Morris, *Phys. Rev. B* **44**, 5322 (1991).
- [73] G.-M. Zhao and D.E. Morris, *Phys. Rev. B* **51**, 16487 (1995); G.-M. Zhao, K.K. Singh, A.P.B. Sinha, and D.E. Morris, *Phys. Rev. B* **52**, 6840 (1995); G.-M. Zhao, M.B. Hunt, H. Keller, and K.A. Müller, *Nature* **385**, 236 (1997).
- [74] M.B. Maple, C.C. Almasan, C.L. Seaman, S.H. Han, *J. Supercond.* **7**, 97 (1994).